

Deep Learning

Lecture 7: Generative adversarial networks

Prof. Gilles Louppe
g.louppe@uliege.be



*Turing Award Won by 3
Pioneers in Artificial Intelligence*



*"ACM named **Yoshua Bengio, Geoffrey Hinton, and Yann LeCun** recipients of the **2018 ACM A.M. Turing Award** for conceptual and engineering breakthroughs that have made deep neural networks a critical component of computing."*

Today

Learn a model of the data.

- Generative adversarial networks
- Wasserstein GANs
- Convergence of GANs
- State of the art
- Applications



Generative adversarial networks

GANs



A two-player game

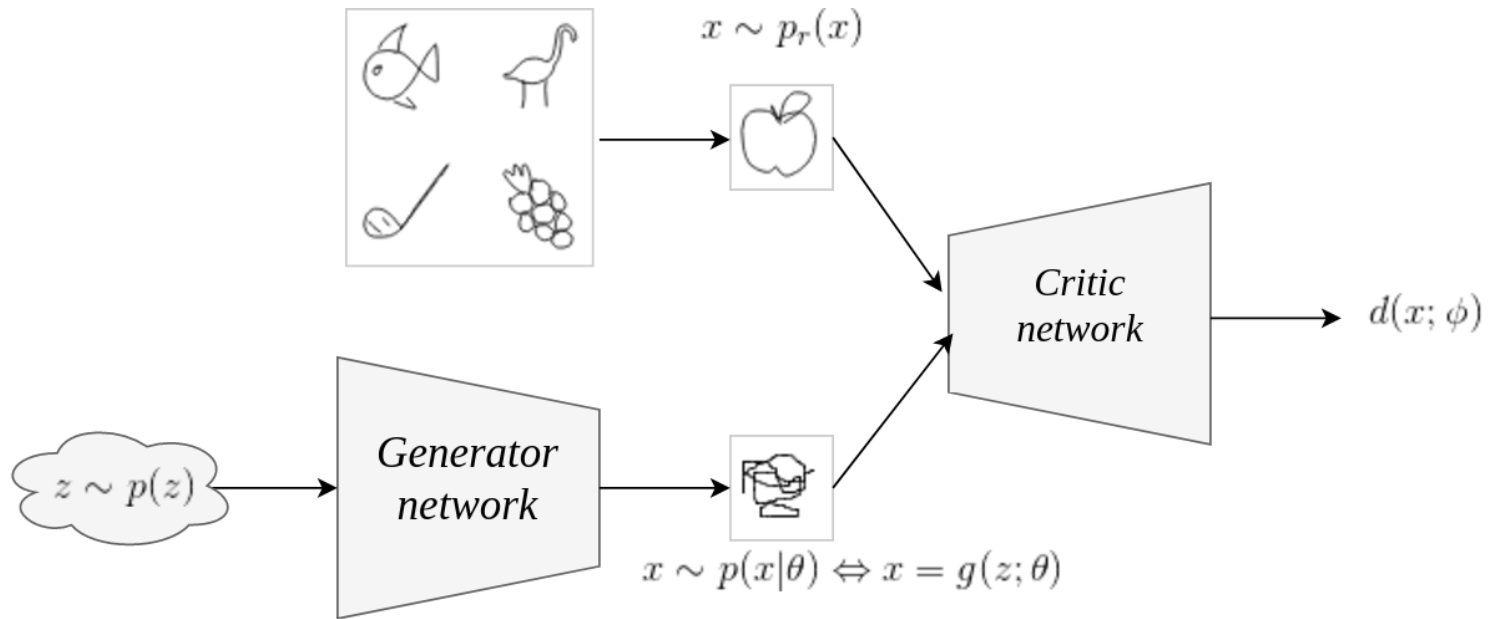
In **generative adversarial networks** (GANs), the task of learning a generative model is expressed as a two-player zero-sum game between two networks.

- The first network is a **generator** $g(\cdot; \theta) : \mathcal{Z} \rightarrow \mathcal{X}$, mapping a latent space equipped with a prior distribution $p(\mathbf{z})$ to the data space, thereby inducing a distribution

$$\mathbf{x} \sim q(\mathbf{x}; \theta) \Leftrightarrow \mathbf{z} \sim p(\mathbf{z}), \mathbf{x} = g(\mathbf{z}; \theta).$$

- The second network $d(\cdot; \phi) : \mathcal{X} \rightarrow [0, 1]$ is a **classifier** trained to distinguish between true samples $\mathbf{x} \sim p(\mathbf{x})$ and generated samples $\mathbf{x} \sim q(\mathbf{x}; \theta)$.

The central mechanism consists in using supervised learning to guide the learning of the generative model.



$$\arg \min_{\theta} \max_{\phi} \underbrace{\mathbb{E}_{\mathbf{x} \sim p(\mathbf{x})} [\log d(\mathbf{x}; \phi)] + \mathbb{E}_{\mathbf{z} \sim p(\mathbf{z})} [\log(1 - d(g(\mathbf{z}; \theta); \phi))]}_{V(\phi, \theta)}$$

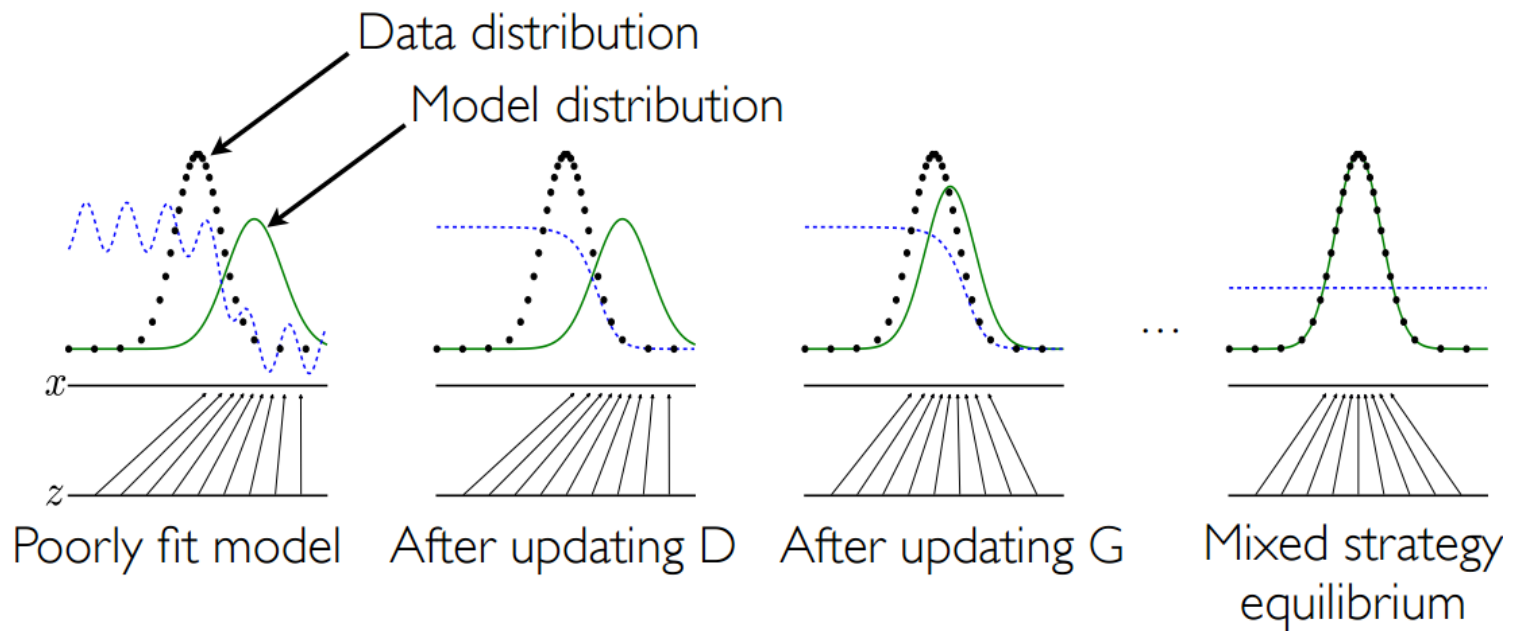
Learning process

In practice, the minimax solution is approximated using [alternating](#) stochastic gradient descent:

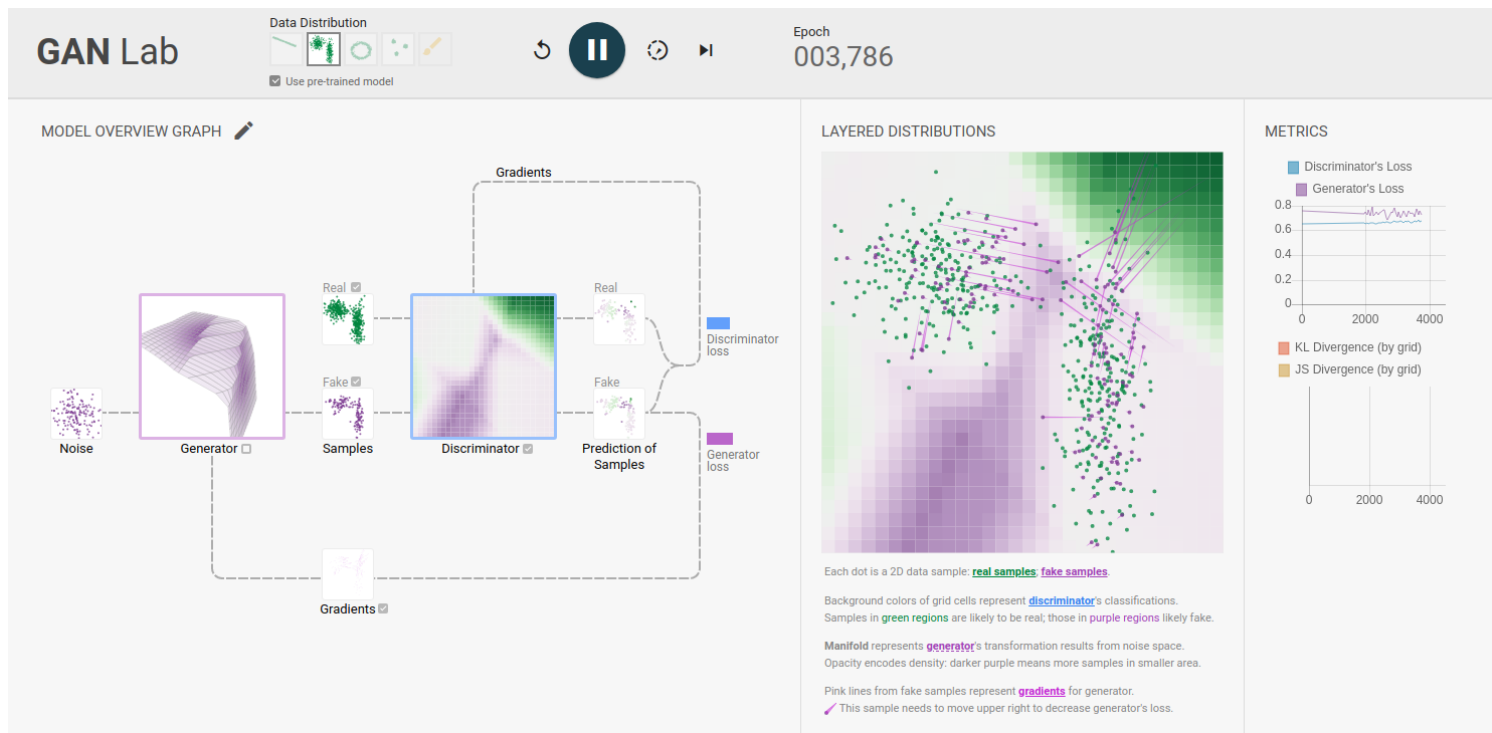
$$\begin{aligned}\theta &\leftarrow \theta - \gamma \nabla_{\theta} V(\phi, \theta) \\ \phi &\leftarrow \phi + \gamma \nabla_{\phi} V(\phi, \theta),\end{aligned}$$

where gradients are estimated with Monte Carlo integration.

- For one step on θ , we can optionally take k steps on ϕ , since we need the classifier to remain near optimal.
- Note that to compute $\nabla_{\theta} V(\phi, \theta)$, it is necessary to backprop all the way through d before computing the partial derivatives with respect to g 's internals.



(Goodfellow et al, 2014)



Demo: GAN Lab

Game analysis

Let us consider value function $V(\phi, \theta)$.

- $V(\phi, \theta)$ is high if d is good at recognizing true from generated samples.
- If d is the best classifier given g , and if V is high, then this implies that the generator is bad at reproducing the data distribution.
- Conversely, g will be a good generative model if V is low when d is a perfect opponent.

Therefore, the ultimate goal is

$$\theta^* = \arg \min_{\theta} \max_{\phi} V(\phi, \theta).$$

For a generator $\textcolor{teal}{g}$ fixed at θ , the classifier $\textcolor{teal}{d}$ with parameters ϕ_θ^* is optimal if and only if

$$\forall \mathbf{x}, d(\mathbf{x}; \phi_\theta^*) = \frac{p(\mathbf{x})}{q(\mathbf{x}; \theta) + p(\mathbf{x})}.$$

Therefore,

$$\begin{aligned} \min_{\theta} \max_{\phi} V(\phi, \theta) &= \min_{\theta} V(\phi_{\theta}^*, \theta) \\ &= \min_{\theta} \mathbb{E}_{\mathbf{x} \sim p(\mathbf{x})} \left[\log \frac{p(\mathbf{x})}{q(\mathbf{x}; \theta) + p(\mathbf{x})} \right] + \mathbb{E}_{\mathbf{x} \sim q(\mathbf{x}; \theta)} \left[\log \frac{q(\mathbf{x}; \theta)}{q(\mathbf{x}; \theta) + p(\mathbf{x})} \right] \\ &= \min_{\theta} \text{KL} \left(p(\mathbf{x}) \parallel \frac{p(\mathbf{x}) + q(\mathbf{x}; \theta)}{2} \right) \\ &\quad + \text{KL} \left(q(\mathbf{x}; \theta) \parallel \frac{p(\mathbf{x}) + q(\mathbf{x}; \theta)}{2} \right) - \log 4 \\ &= \min_{\theta} 2 \text{JSD}(p(\mathbf{x}) \parallel q(\mathbf{x}; \theta)) - \log 4 \end{aligned}$$

where **JSD** is the Jensen-Shannon divergence.

In summary,

$$\begin{aligned}\theta^* &= \arg \min_{\theta} \max_{\phi} V(\phi, \theta) \\ &= \arg \min_{\theta} \text{JSD}(p(\mathbf{x}) || q(\mathbf{x}; \theta)).\end{aligned}$$

Since $\text{JSD}(p(\mathbf{x}) || q(\mathbf{x}; \theta))$ is minimum if and only if

$$p(\mathbf{x}) = q(\mathbf{x}; \theta)$$

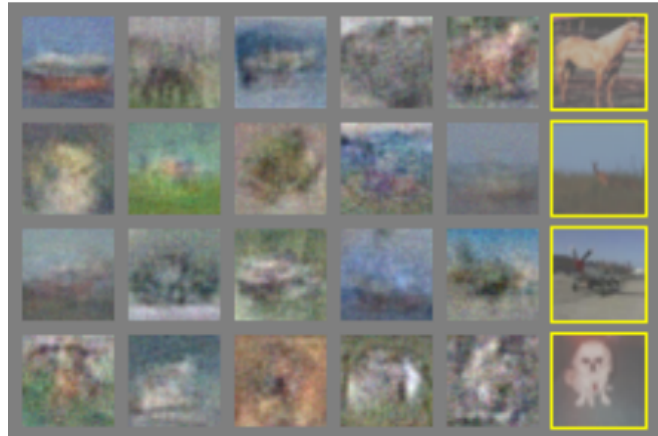
for all \mathbf{x} , this proves that the minimax solution corresponds to a generative model that perfectly reproduces the true data distribution.



a)



b)



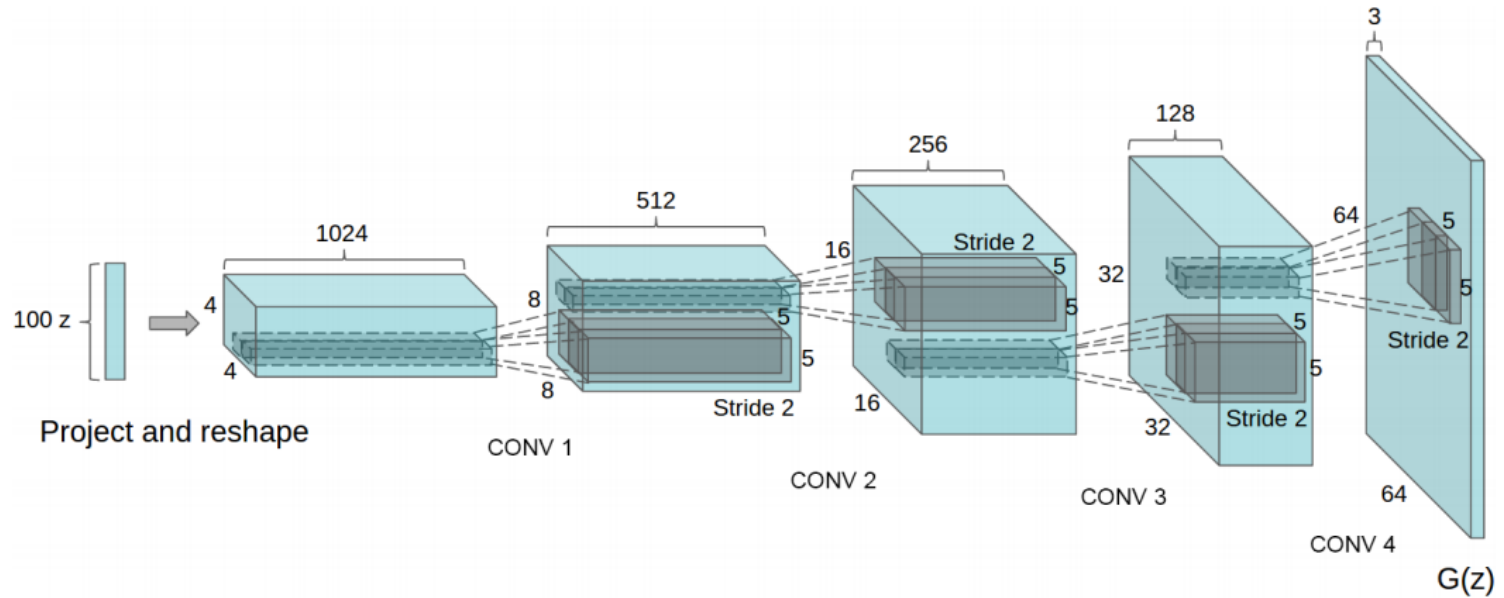
c)



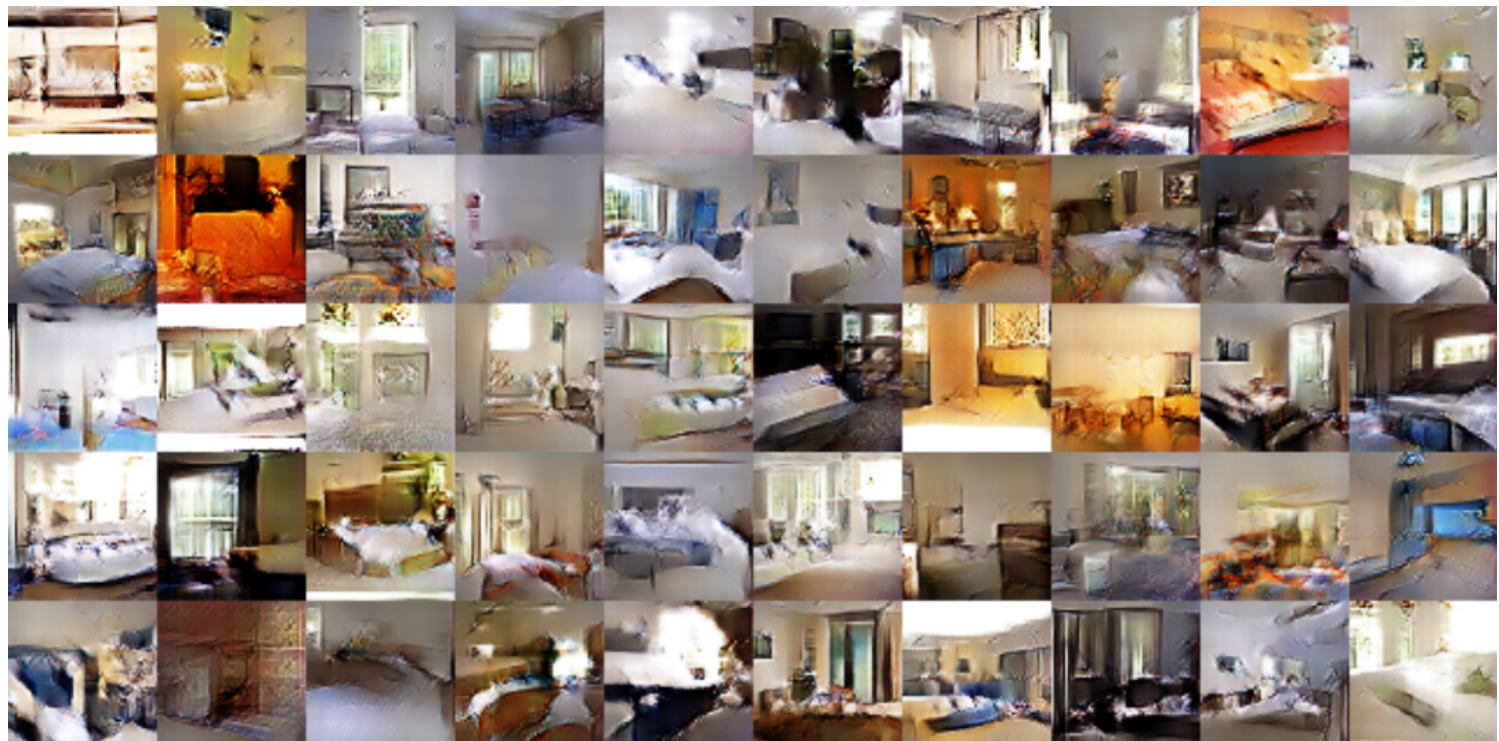
d)

(Goodfellow et al, 2014)

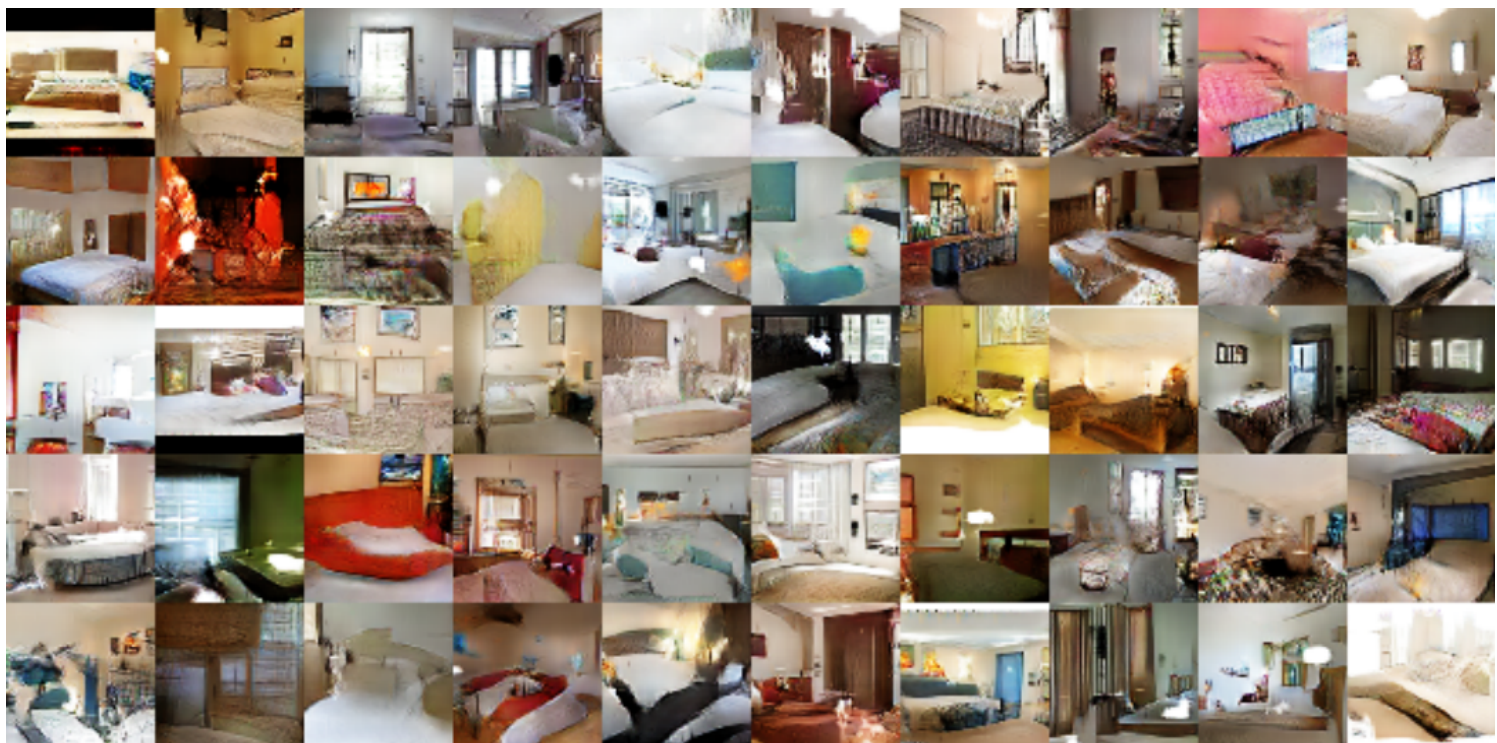
DCGANs



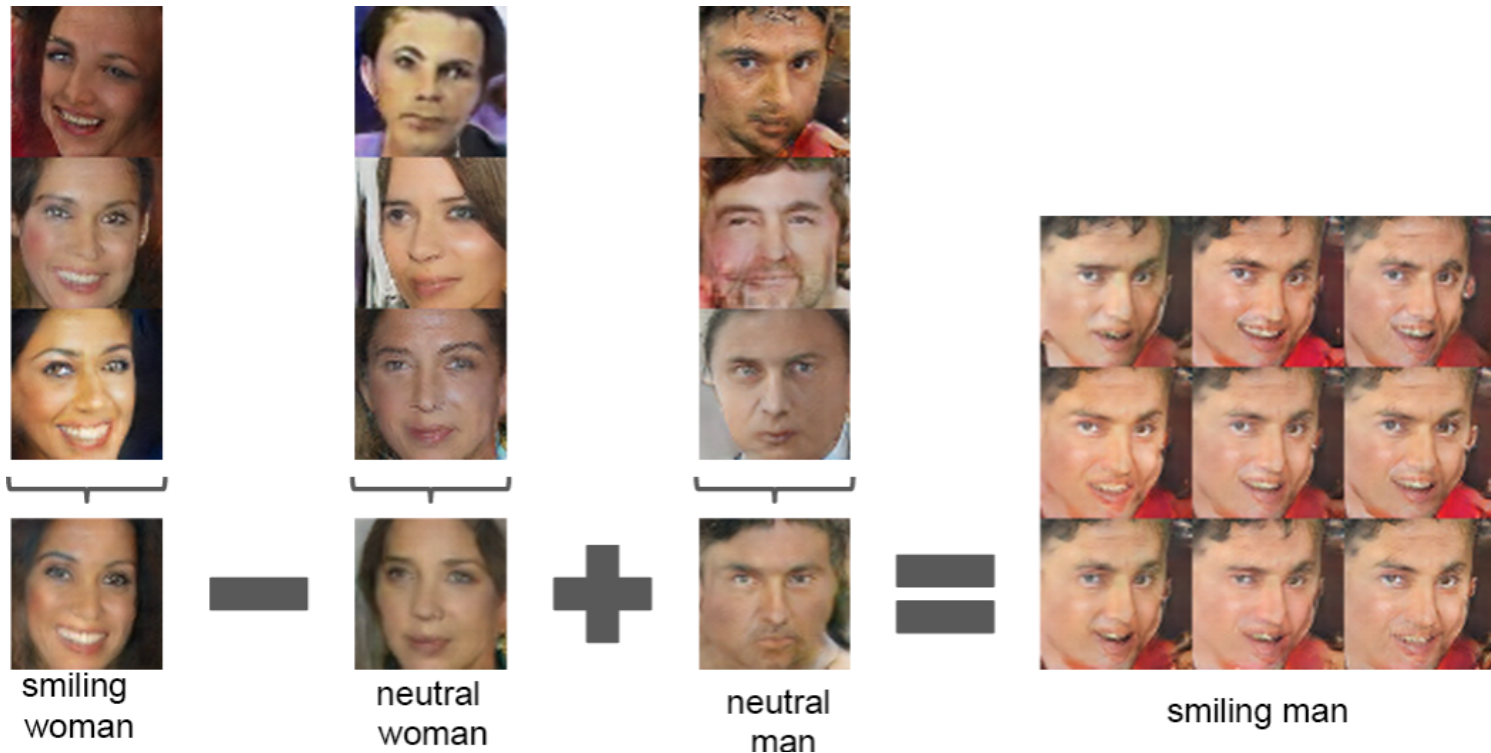
(Radford et al, 2015)



(Radford et al, 2015)



(Radford et al, 2015)

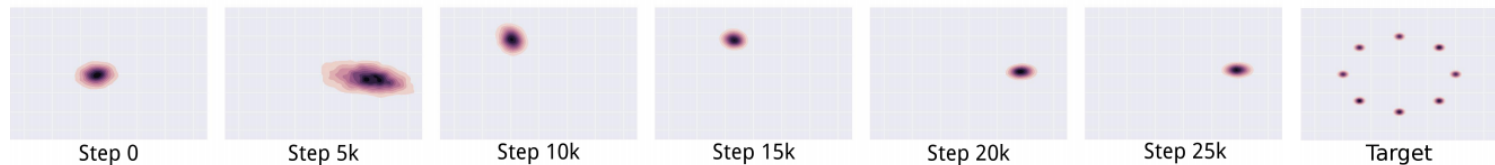


Vector arithmetic in latent space (Radford et al, 2015)

Open problems

Training a standard GAN often results in pathological behaviors:

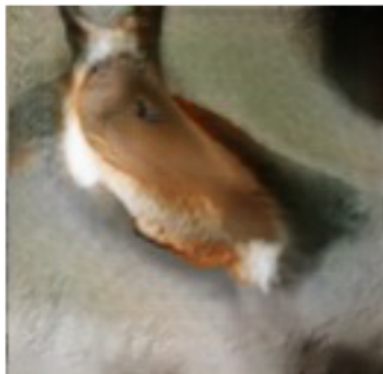
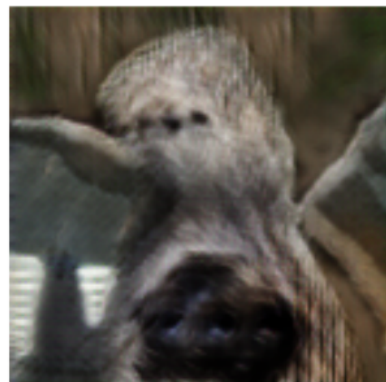
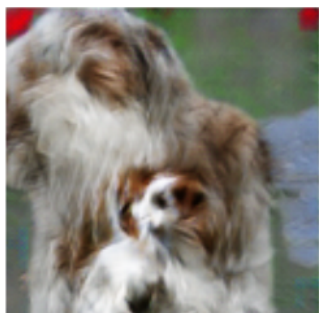
- **Oscillations** without convergence: contrary to standard loss minimization, alternating stochastic gradient descent has no guarantee of convergence.
- **Vanishing gradients**: when the classifier d is too good, the value function saturates and we end up with no gradient to update the generator (more on this later).
- **Mode collapse**: the generator g models very well a small sub-population, concentrating on a few modes of the data distribution.
- Performance is also difficult to assess in practice.



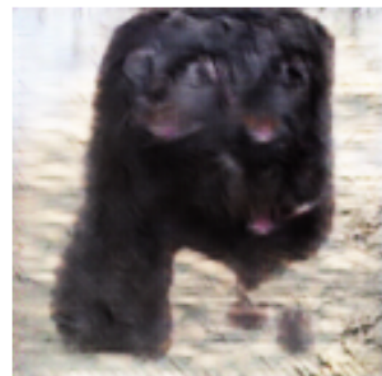
Mode collapse (Metz et al, 2016)

Cabinet of curiosities

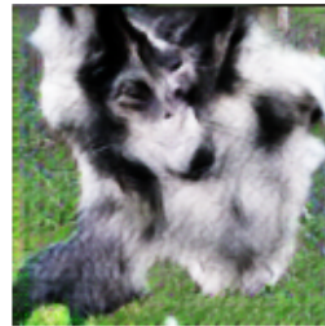
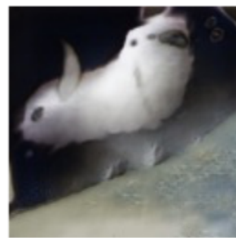
While early results (2014-2016) were already impressive, a close inspection of the fake samples distribution $q(\mathbf{x}; \theta)$ often revealed fundamental issues highlighting architectural limitations.



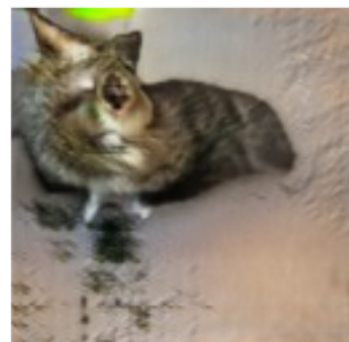
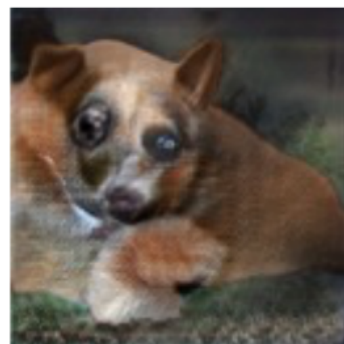
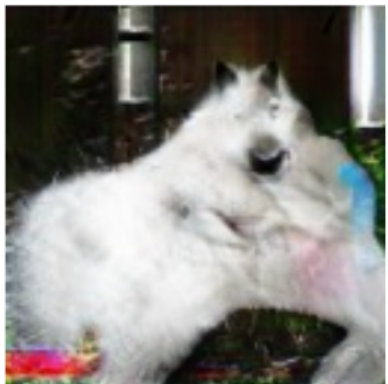
Cherry-picks (Goodfellow, 2016)



Problems with counting (Goodfellow, 2016)



Problems with perspective (Goodfellow, 2016)



Problems with global structures (Goodfellow, 2016)

Wasserstein GANs

Return of the Vanishing Gradients

For most non-toy data distributions, the fake samples $\mathbf{x} \sim q(\mathbf{x}; \theta)$ may be so bad initially that the response of d saturates.

At the limit, when d is perfect given the current generator g ,

$$\begin{aligned} d(\mathbf{x}; \phi) &= 1, \forall \mathbf{x} \sim p(\mathbf{x}), \\ d(\mathbf{x}; \phi) &= 0, \forall \mathbf{x} \sim q(\mathbf{x}; \theta). \end{aligned}$$

Therefore,

$$V(\phi, \theta) = \mathbb{E}_{\mathbf{x} \sim p(\mathbf{x})} [\log d(\mathbf{x}; \phi)] + \mathbb{E}_{\mathbf{z} \sim p(\mathbf{z})} [\log(1 - d(g(\mathbf{z}; \theta); \phi))] = 0$$

and $\nabla_{\theta} V(\phi, \theta) = 0$, thereby **halting** gradient descent.

Dilemma

- If d is bad, then g does not have accurate feedback and the loss function cannot represent the reality.
- If d is too good, the gradients drop to 0, thereby slowing down or even halting the optimization.

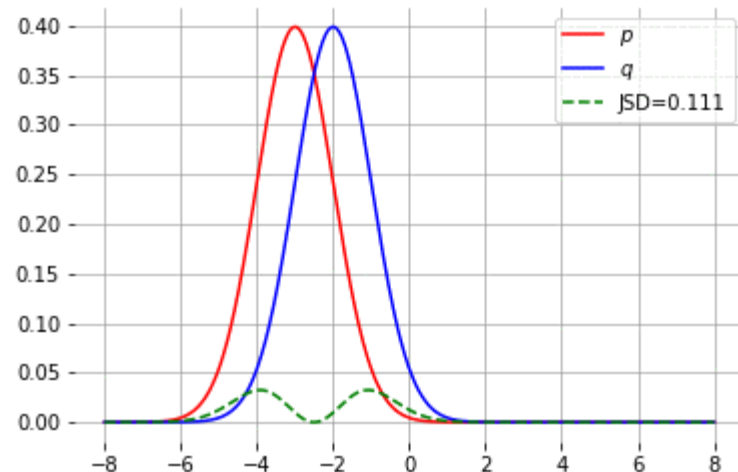
Jensen-Shannon divergence

For any two distributions p and q ,

$$0 \leq JSD(p||q) \leq \log 2,$$

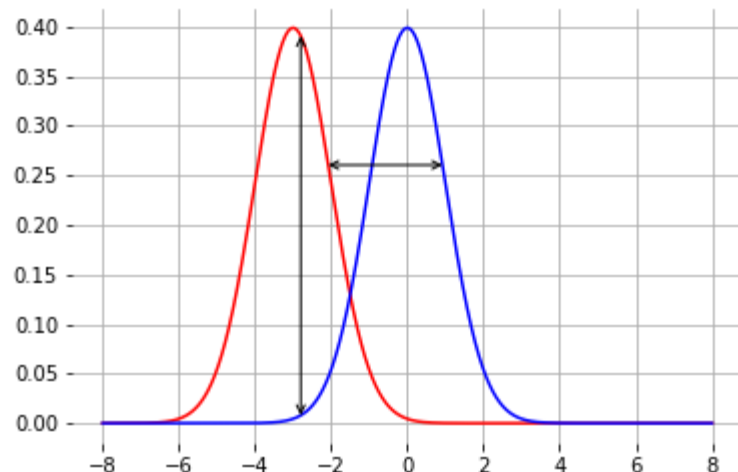
where

- $JSD(p||q) = 0$ if and only if $p = q$,
- $JSD(p||q) = \log 2$ if and only if p and q have disjoint supports.



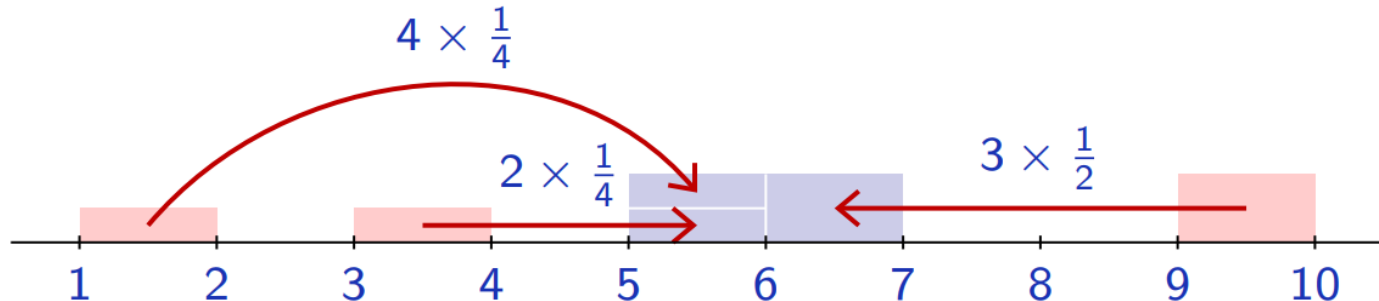
Notice how the Jensen-Shannon divergence poorly accounts for the metric structure of the space.

Intuitively, instead of comparing distributions "vertically", we would like to compare them "horizontally".



Wasserstein distance

An alternative choice is the **Earth mover's distance**, which intuitively corresponds to the minimum mass displacement to transform one distribution into the other.



- $p = \frac{1}{4}\mathbf{1}_{[1,2]} + \frac{1}{4}\mathbf{1}_{[3,4]} + \frac{1}{2}\mathbf{1}_{[9,10]}$
- $q = \mathbf{1}_{[5,7]}$

Then,

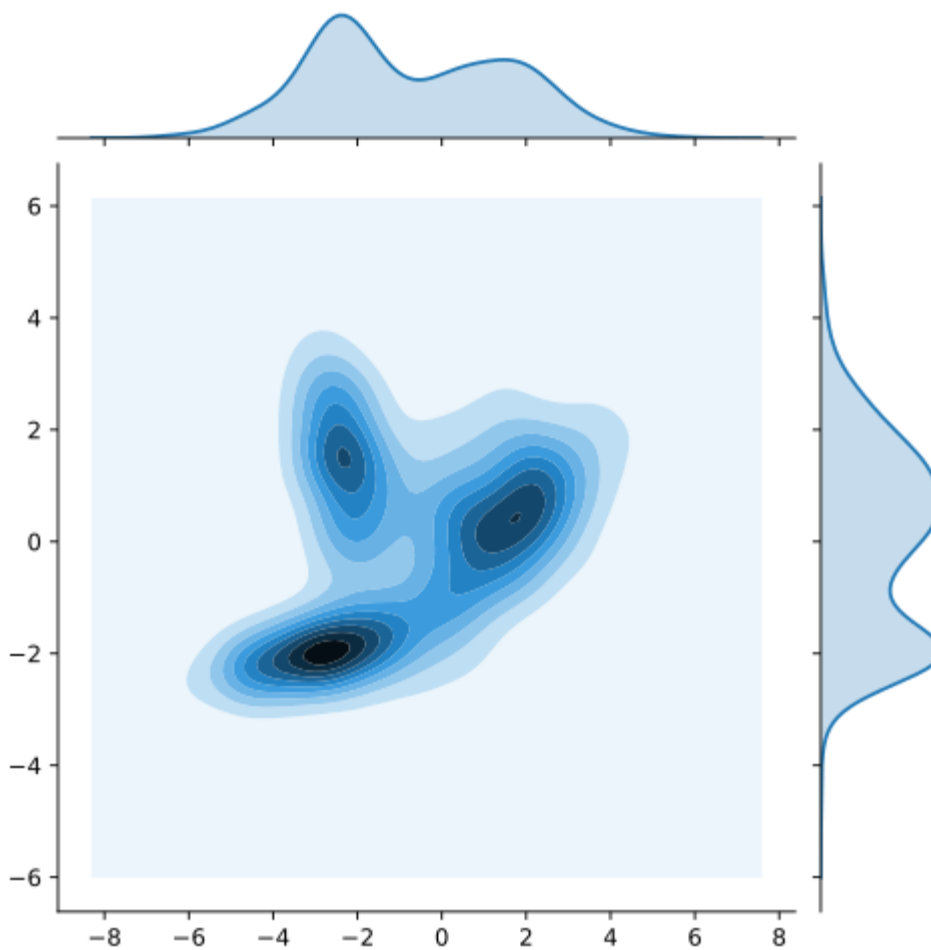
$$W_1(p, q) = 4 \times \frac{1}{4} + 2 \times \frac{1}{4} + 3 \times \frac{1}{2} = 3$$

The Earth mover's distance is also known as the Wasserstein-1 distance and is defined as:

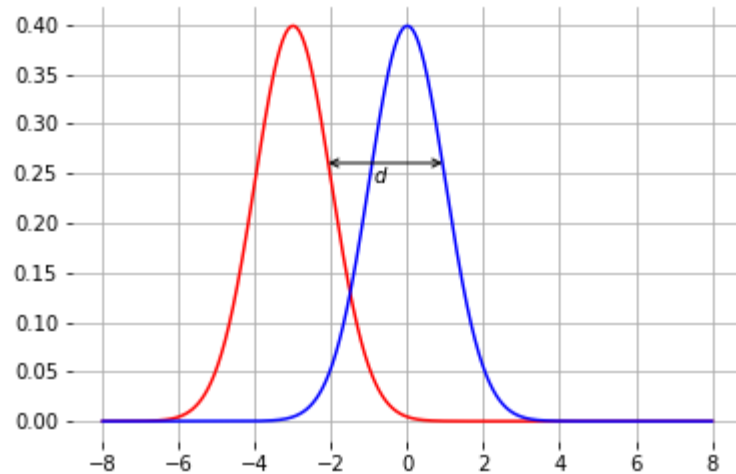
$$W_1(p, q) = \inf_{\gamma \in \Pi(p, q)} \mathbb{E}_{(x, y) \sim \gamma} [| |x - y| |]$$

where:

- $\Pi(p, q)$ denotes the set of all joint distributions $\gamma(x, y)$ whose marginals are respectively p and q ;
- $\gamma(x, y)$ indicates how much mass must be transported from x to y in order to transform the distribution p into q .
- $| | \cdot | |$ is the L1 norm and $| |x - y| |$ represents the cost of moving a unit of mass from x to y .



Notice how the W_1 distance does not saturate. Instead, it increases monotonically with the distance between modes:



$$W_1(p, q) = d$$

For any two distributions p and q ,

- $W_1(p, q) \in \mathbb{R}^+$,
- $W_1(p, q) = 0$ if and only if $p = q$.

Wasserstein GANs

Given the attractive properties of the Wasserstein-1 distance, Arjovsky et al (2017) propose to learn a generative model by solving instead:

$$\theta^* = \arg \min_{\theta} W_1(p(\mathbf{x}) || q(\mathbf{x}; \theta))$$

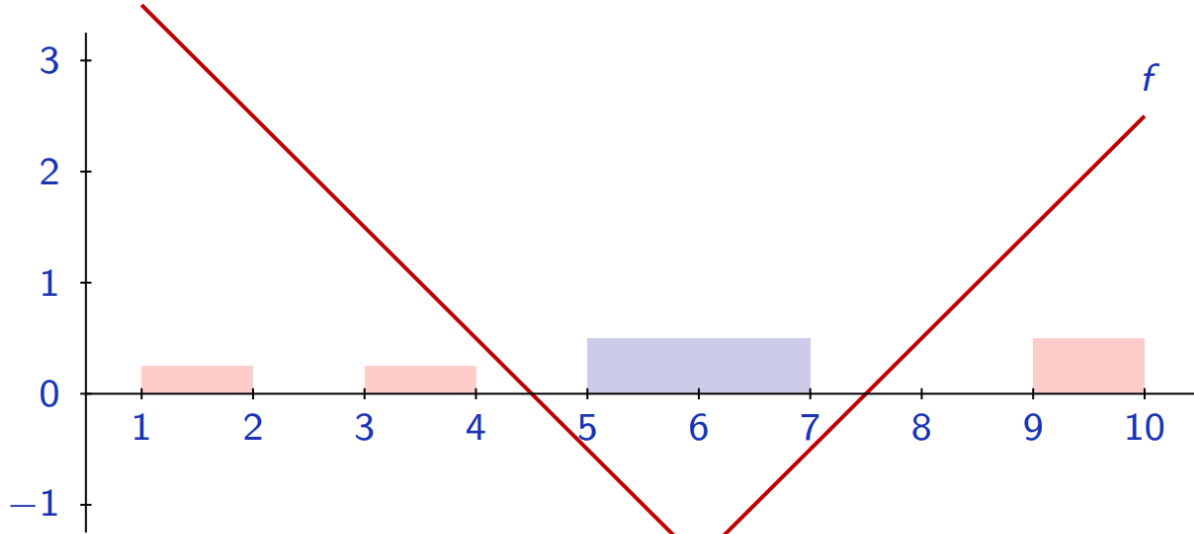
Unfortunately, the definition of W_1 does not provide with an operational way of estimating it because of the intractable \inf .

On the other hand, the Kantorovich-Rubinstein duality tells us that

$$W_1(p(\mathbf{x}) || q(\mathbf{x}; \theta)) = \sup_{\|f\|_L \leq 1} \mathbb{E}_{\mathbf{x} \sim p(\mathbf{x})} [f(\mathbf{x})] - \mathbb{E}_{\mathbf{x} \sim q(\mathbf{x}; \theta)} [f(\mathbf{x})]$$

where the supremum is over all the 1-Lipschitz functions $f : \mathcal{X} \rightarrow \mathbb{R}$. That is, functions f such that

$$\|f\|_L = \max_{\mathbf{x}, \mathbf{x}'} \frac{\|f(\mathbf{x}) - f(\mathbf{x}')\|}{\|\mathbf{x} - \mathbf{x}'\|} \leq 1.$$



For $p = \frac{1}{4}\mathbf{1}_{[1,2]} + \frac{1}{4}\mathbf{1}_{[3,4]} + \frac{1}{2}\mathbf{1}_{[9,10]}$ and $q = \mathbf{1}_{[5,7]}$,

$$\begin{aligned}
 W_1(p, q) &= 4 \times \frac{1}{4} + 2 \times \frac{1}{4} + 3 \times \frac{1}{2} = 3 \\
 &= \underbrace{\left(3 \times \frac{1}{4} + 1 \times \frac{1}{4} + 2 \times \frac{1}{2}\right)}_{\mathbb{E}_{\mathbf{x} \sim p(\mathbf{x})}[f(\mathbf{x})]} - \underbrace{\left(-1 \times \frac{1}{2} - 1 \times \frac{1}{2}\right)}_{\mathbb{E}_{\mathbf{x} \sim q(\mathbf{x}; \theta)}[f(\mathbf{x})]} = 3
 \end{aligned}$$

Using this result, the Wasserstein GAN algorithm consists in solving the minimax problem:

$$\theta^* = \arg \min_{\theta} \max_{\phi: \|d(\cdot; \phi)\|_L \leq 1} \mathbb{E}_{\mathbf{x} \sim p(\mathbf{x})} [d(\mathbf{x}; \phi)] - \mathbb{E}_{\mathbf{x} \sim q(\mathbf{x}; \theta)} [d(\mathbf{x}; \phi)]$$

Note that this formulation is very close to the original GANs, except that:

- The classifier $d : \mathcal{X} \rightarrow [0, 1]$ is replaced by a critic function $d : \mathcal{X} \rightarrow \mathbb{R}$ and its output is not interpreted through the cross-entropy loss;
- There is a strong regularization on the form of d . In practice, to ensure 1-Lipschitzness,
 - Arjovsky et al (2017) propose to clip the weights of the critic at each iteration;
 - Gulrajani et al (2017) add a regularization term to the loss.
- As a result, Wasserstein GANs benefit from:
 - a meaningful loss metric,
 - improved stability (no mode collapse is observed).

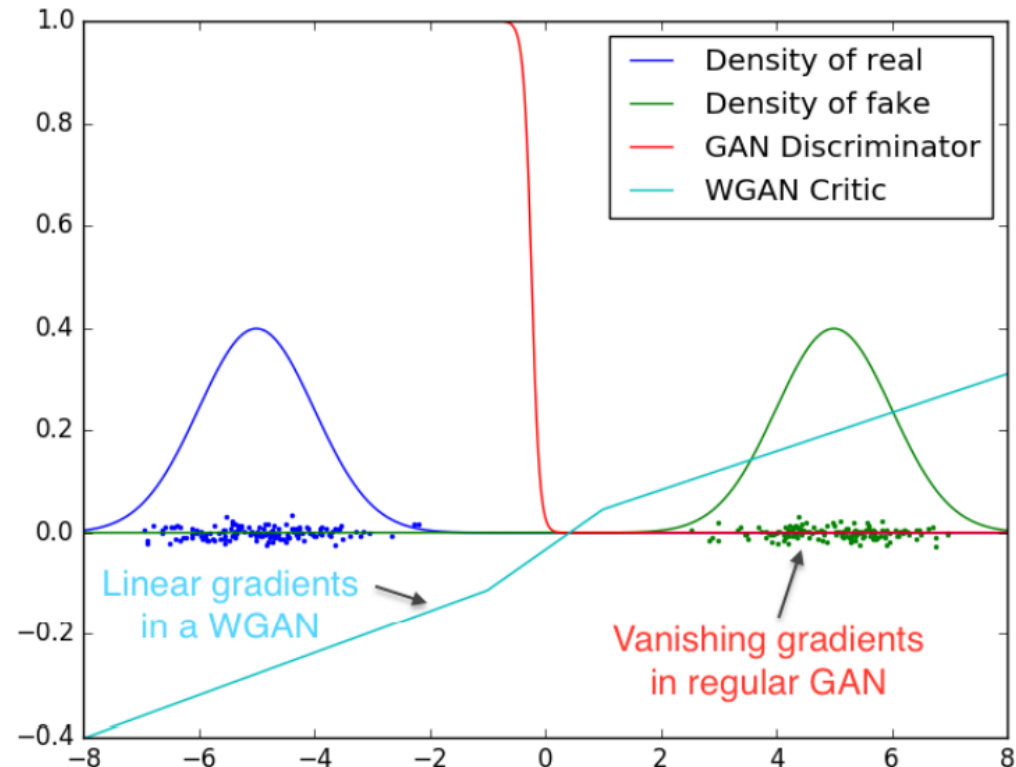
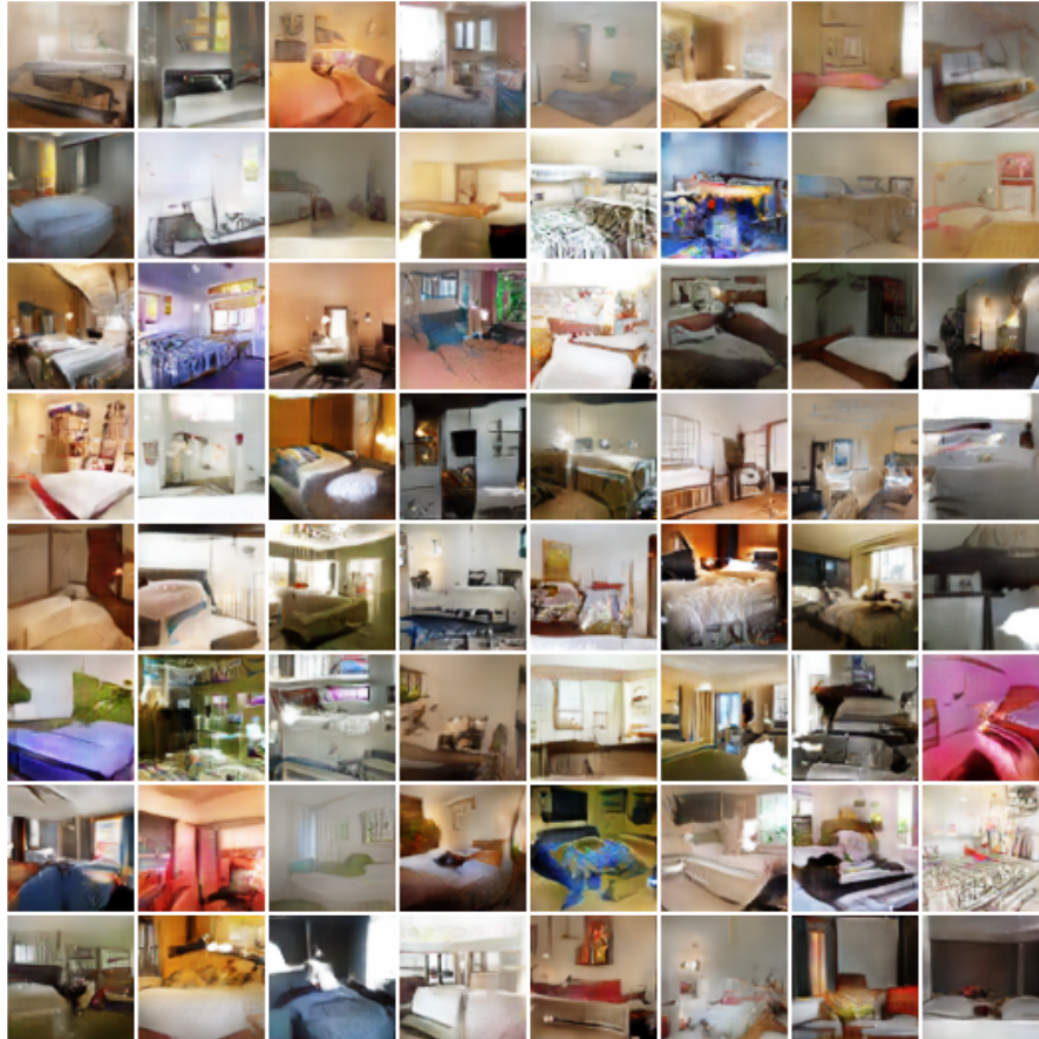


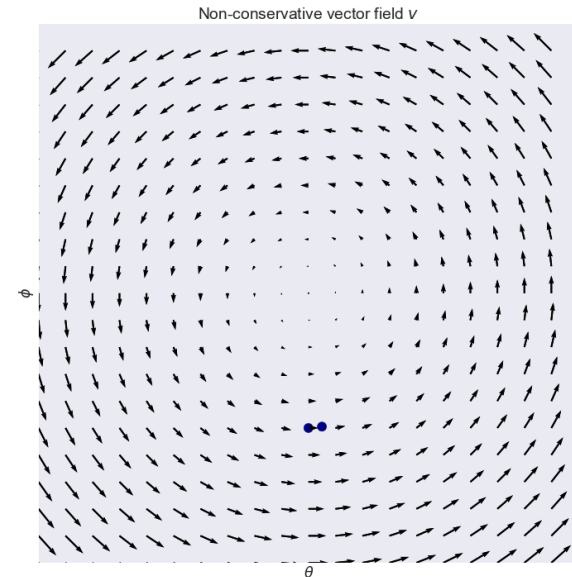
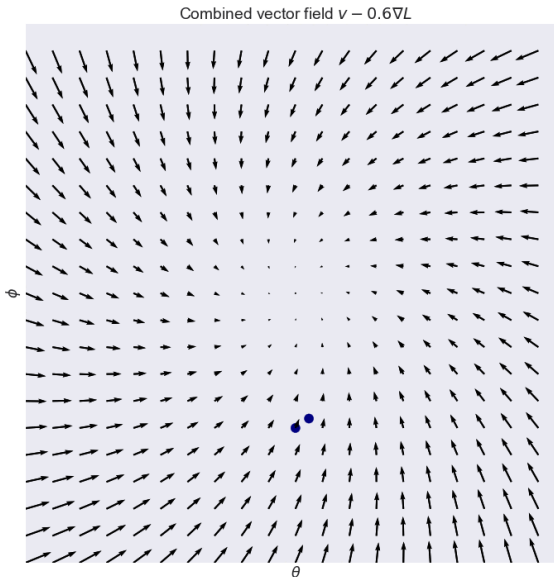
Figure 2: Optimal discriminator and critic when learning to differentiate two Gaussians. As we can see, the discriminator of a minimax GAN saturates and results in vanishing gradients. Our WGAN critic provides very clean gradients on all parts of the space.

(Arjovsky et al, 2017)



(Arjovsky et al, 2017)

Convergence of GANs



Solving for saddle points is different from gradient descent.

- Minimization problems yield **conservative** vector fields.
- Min-max saddle point problems may yield **non-conservative** vector fields.

Following the notations of Mescheder et al (2018), the training objective for the two players can be described by an objective function of the form

$$L(\theta, \phi) = \mathbb{E}_{p(\mathbf{z})} [f(d(g(\mathbf{z}; \theta); \phi))] + \mathbb{E}_{p(\mathbf{x})} [f(-d(\mathbf{x}; \phi))],$$

where the goal of the generator is to minimizes the loss, whereas the discriminator tries to maximize it.

- If $f(t) = -\log(1 + \exp(-t))$, then we recover the original GAN objective.
- if $f(t) = -t$ and if we impose the Lipschitz constraint on d , then we recover Wassterstein GAN.

Training algorithms can be described as fixed points algorithms that apply some operator $F_h(\theta, \phi)$ to the parameters values (θ, ϕ) .

- For simultaneous gradient descent,

$$F_h(\theta, \phi) = (\theta, \phi) + h v(\theta, \phi)$$

where $v(\theta, \phi)$ denotes the **gradient vector field**

$$v(\theta, \phi) := \begin{pmatrix} -\nabla_{\theta} L(\theta, \phi) \\ \nabla_{\phi} L(\theta, \phi) \end{pmatrix}.$$

- Similarly, alternating gradient descent can be described by an operator $F_h = F_{2,h} \circ F_{1,h}$, where $F_{1,h}$ and $F_{2,h}$ perform an update for the generator and discriminator, respectively.

Local convergence near an equilibrium point

Let us consider the Jacobian $F'_h(\theta^*, \phi^*)$ at the equilibrium (θ^*, ϕ^*) :

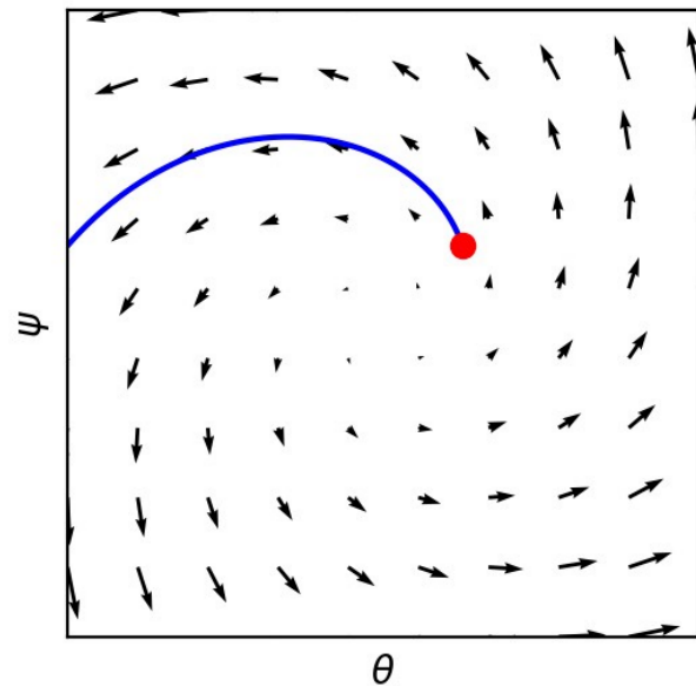
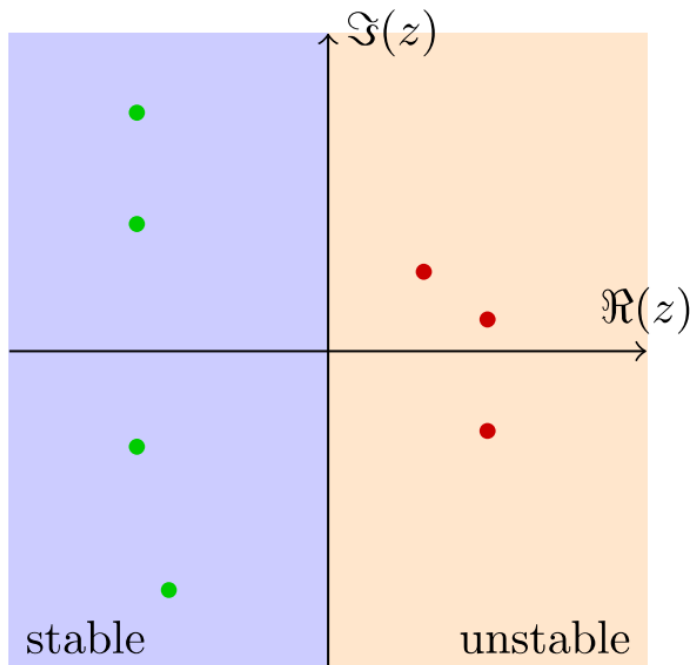
- if $F'_h(\theta^*, \phi^*)$ has eigenvalues with absolute value bigger than 1, the training will generally not converge to (θ^*, ϕ^*) .
- if all eigenvalues have absolute value smaller than 1, the training will converge to (θ^*, ϕ^*) .
- if all eigenvalues values are on the unit circle, training can be convergent, divergent or neither.

For the (idealized) continuous system

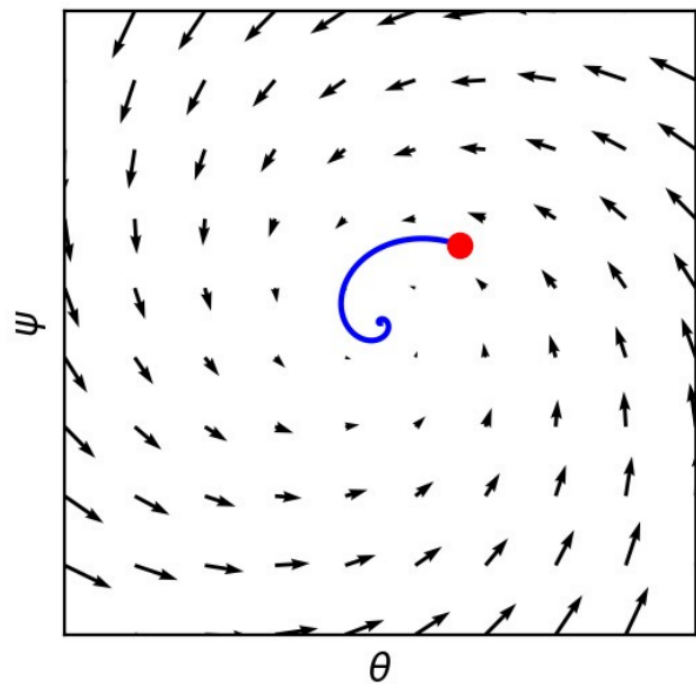
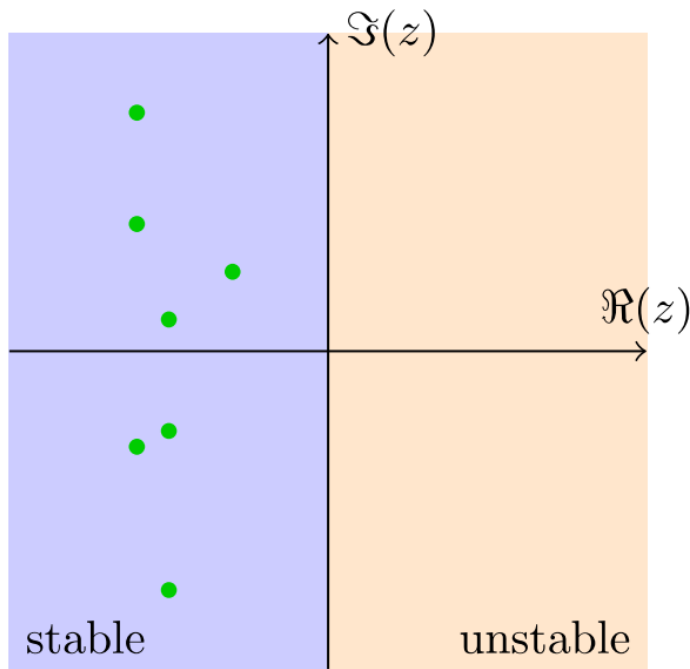
$$\begin{pmatrix} \dot{\theta}(t) \\ \dot{\phi}(t) \end{pmatrix} = \begin{pmatrix} -\nabla_{\theta}L(\theta, \phi) \\ \nabla_{\phi}L(\theta, \phi) \end{pmatrix},$$

which corresponds to training GANs with infinitely small learning rate:

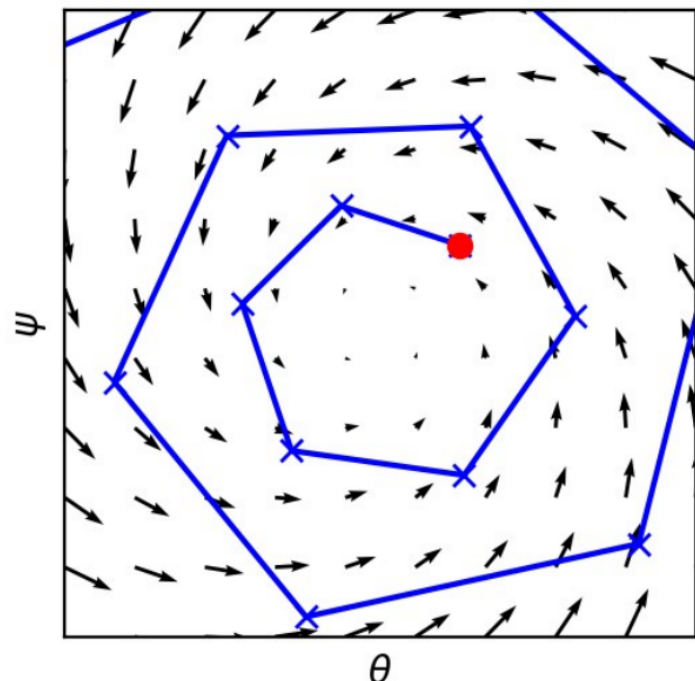
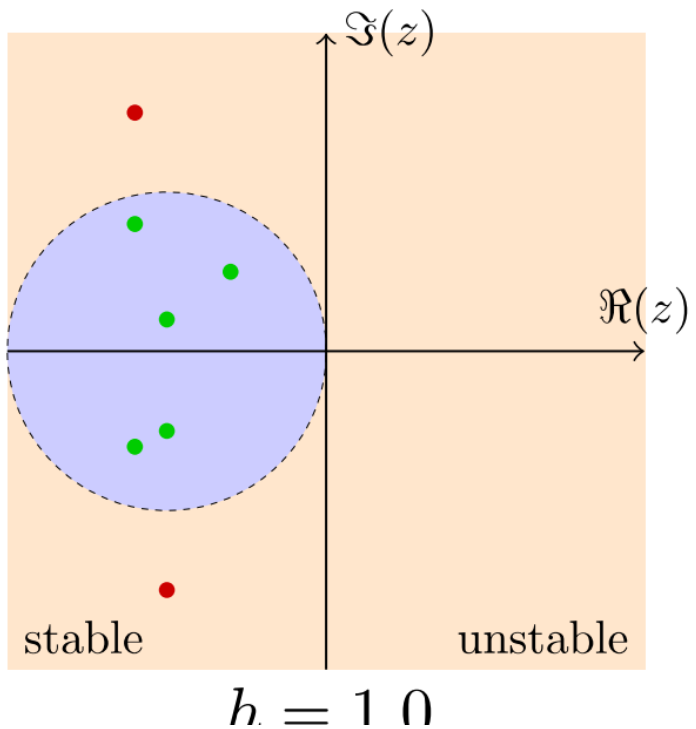
- if all eigenvalues of the Jacobian $v'(\theta^*, \phi^*)$ at a stationary point (θ^*, ϕ^*) have negative real-part, the continuous system converges locally to (θ^*, ϕ^*) ;
- if $v'(\theta^*, \phi^*)$ has eigenvalues with positive real-part, the continuous system is not locally convergent.
- if all eigenvalues have zero real-part, it can be convergent, divergent or neither.



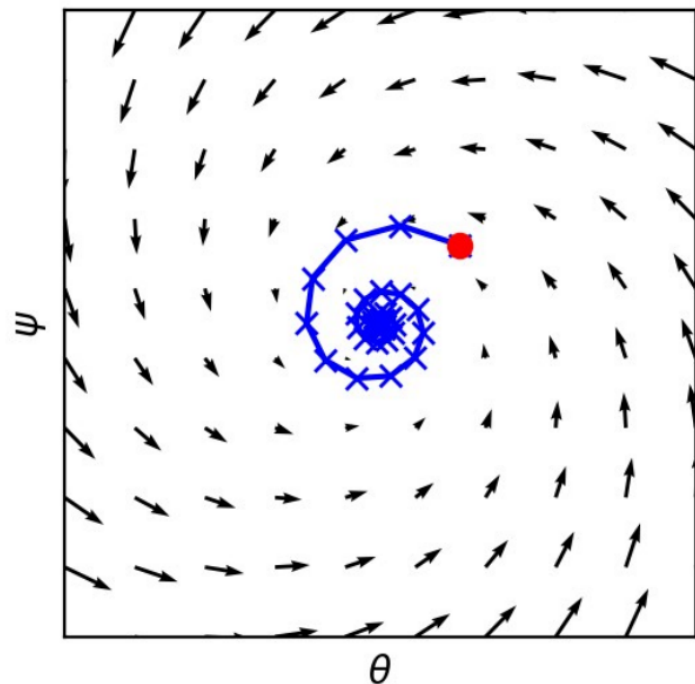
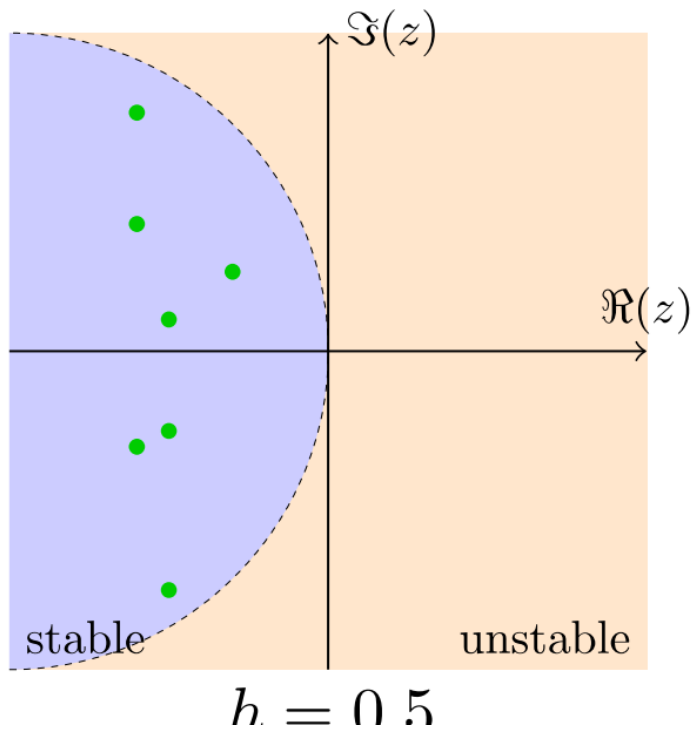
Continuous system: divergence.



Continuous system: convergence.

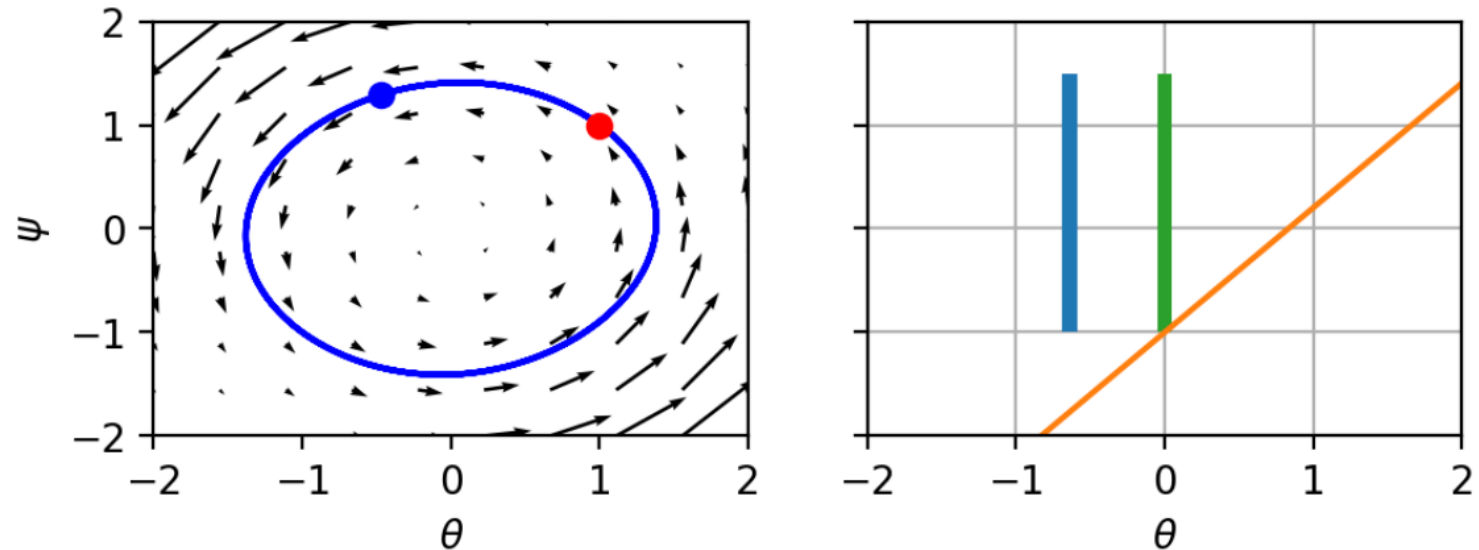


Discrete system: divergence.



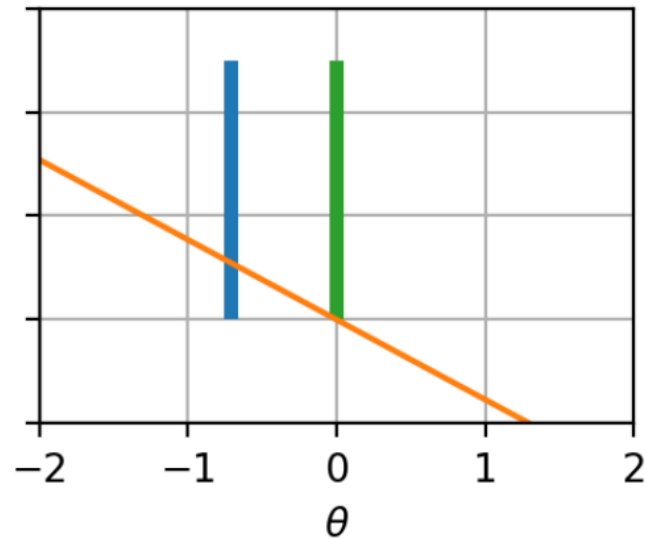
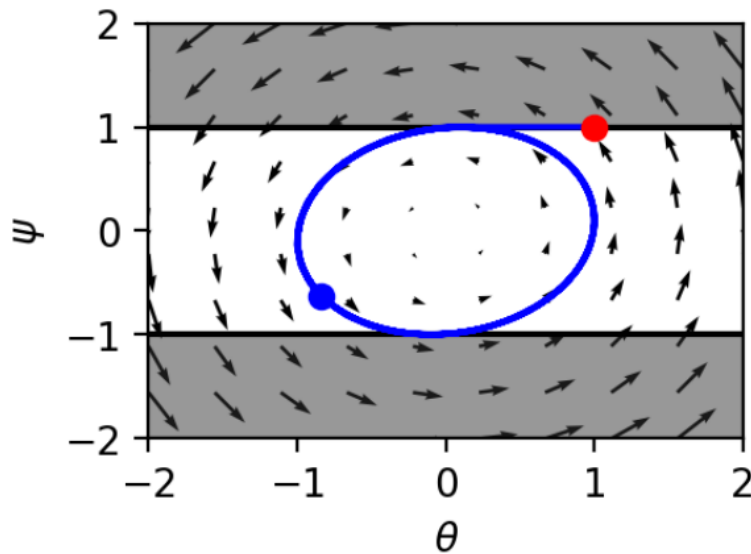
Discrete system: convergence.

Dirac-GAN: Vanilla GANs



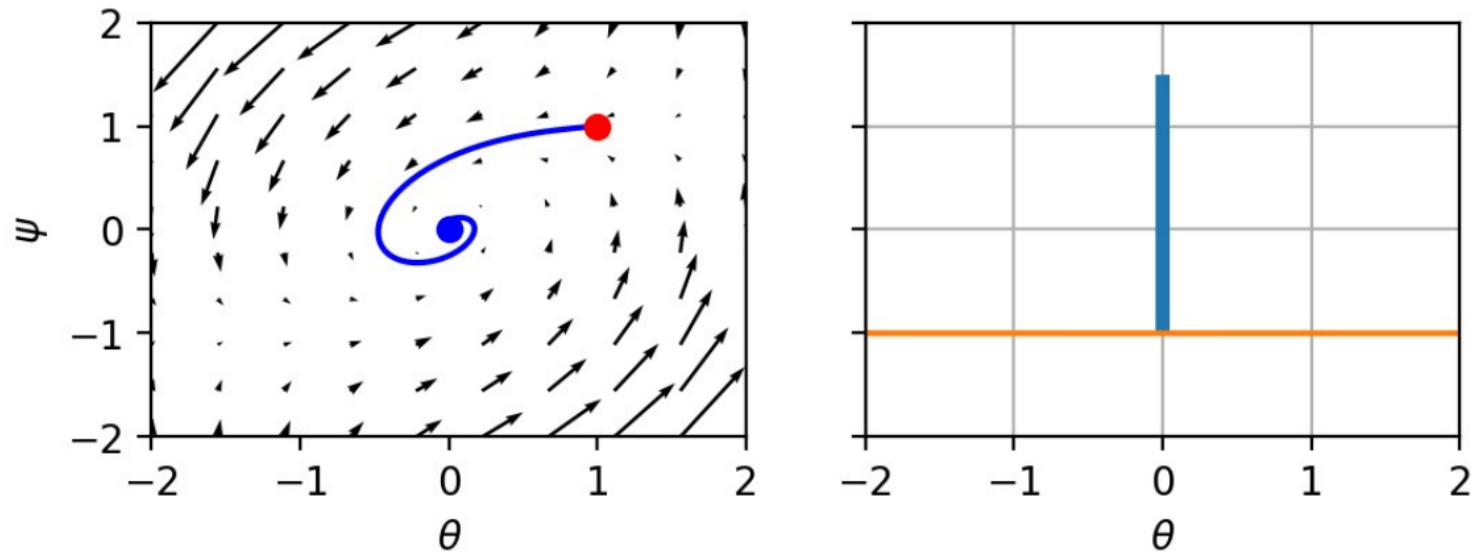
On the Dirac-GAN toy problem, eigenvalues are $\{-f'(0)i, +f'(0)i\}$. Therefore convergence is not guaranteed.

Dirac-GAN: Wasserstein GANs



Eigenvalues are $\{-i, +i\}$. Therefore convergence is not guaranteed.

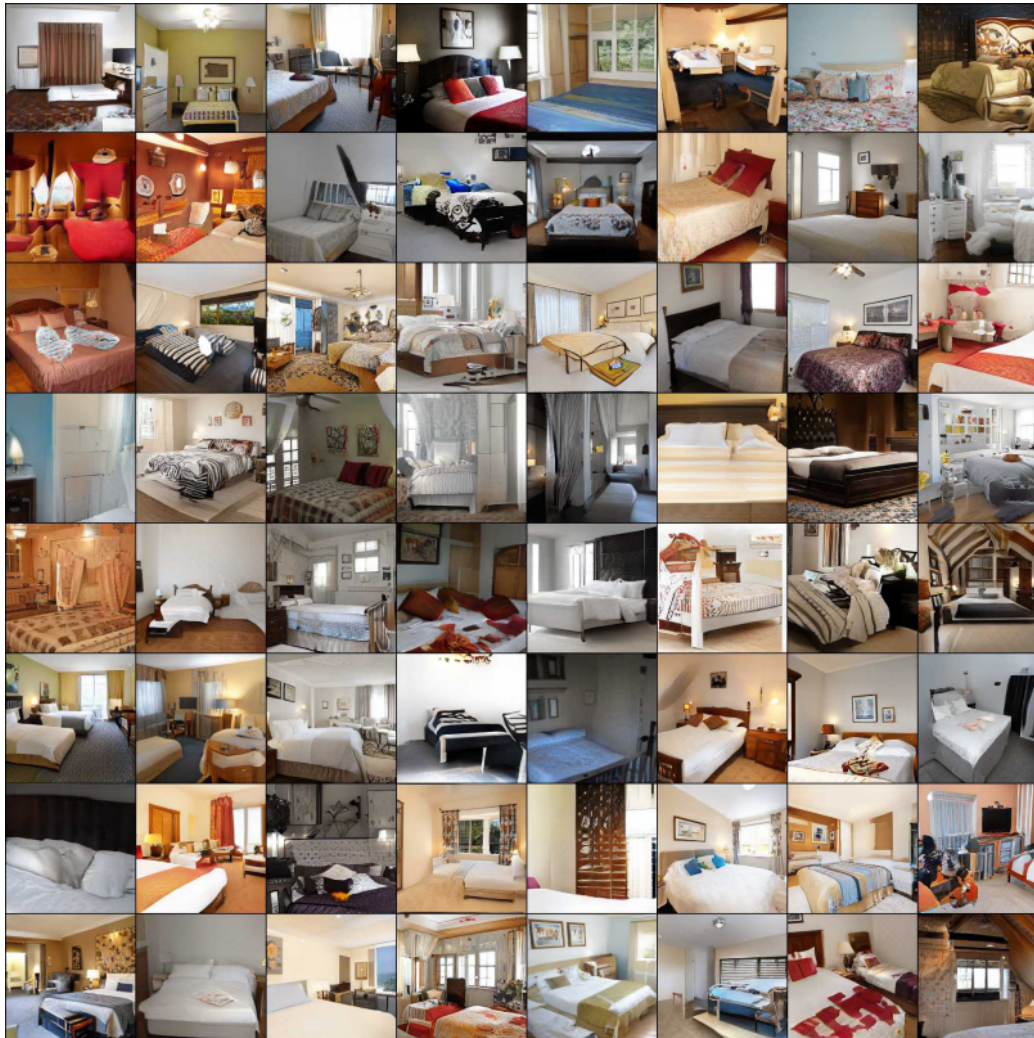
Dirac-GAN: Zero-centered gradient penalties



A penalty on the squared norm of the gradients of the discriminator results in the regularization

$$R_1(\phi) = \frac{\gamma}{2} \mathbb{E}_{\mathbf{x} \sim p(\mathbf{x})} [||\nabla_{\mathbf{x}} d(\mathbf{x}; \phi)||^2].$$

The resulting eigenvalues are $\{-\frac{\gamma}{2} \pm \sqrt{\frac{\gamma}{4} - f'(0)^2}\}$. Therefore, for $\gamma > 0$, all eigenvalues have negative real part, hence training is locally convergent!







State of the art



Ian Goodfellow

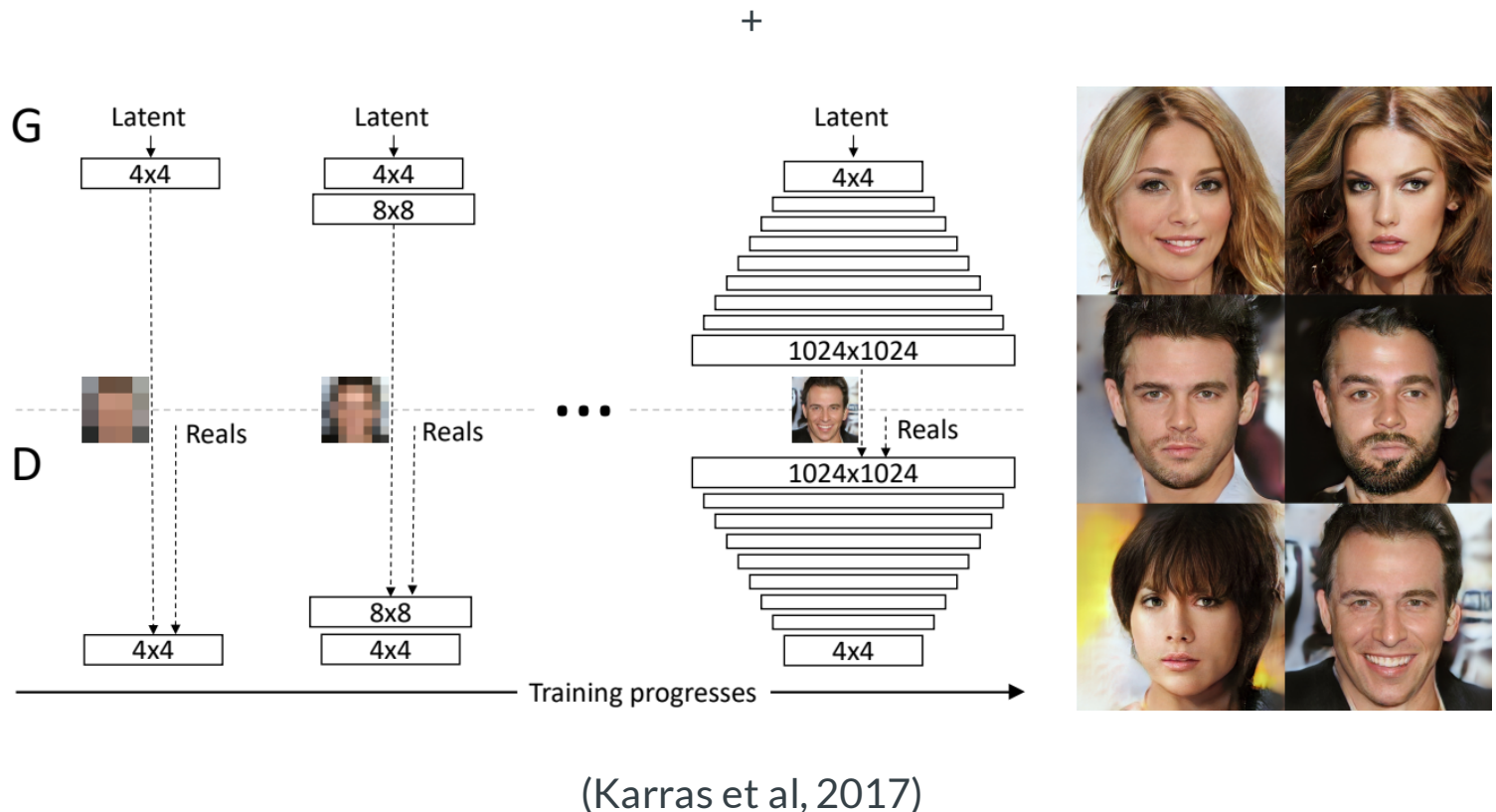
@goodfellow_ian

4.5 years of GAN progress on face generation. arxiv.org/abs/1406.2661
arxiv.org/abs/1511.06434
arxiv.org/abs/1606.07536
arxiv.org/abs/1710.10196
arxiv.org/abs/1812.04948



Progressive growing of GANs

Wasserstein GANs as baseline (Arjovsky et al, 2017) +
Gradient Penalty (Gulrajani, 2017) + (quite a few other tricks)



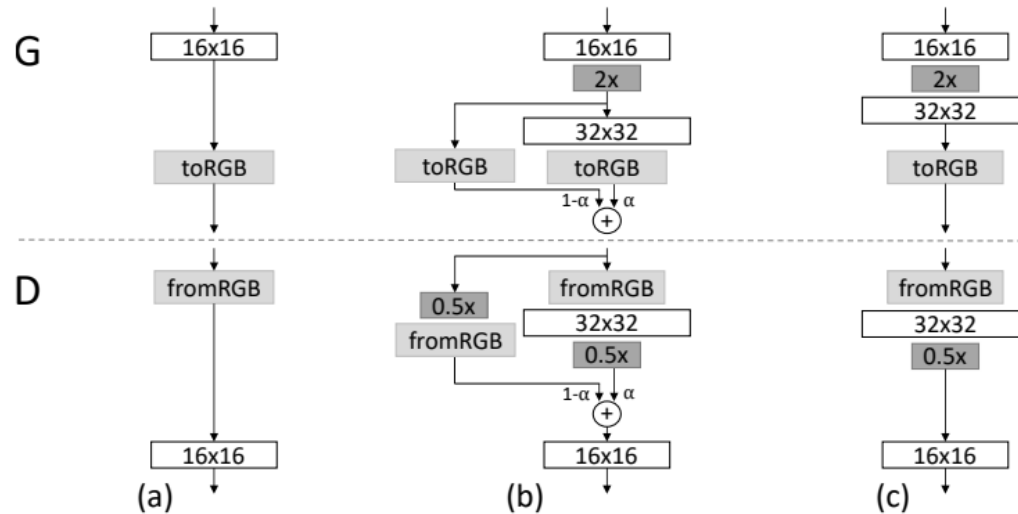


Figure 2: When doubling the resolution of the generator (G) and discriminator (D) we fade in the new layers smoothly. This example illustrates the transition from 16×16 images (a) to 32×32 images (c). During the transition (b) we treat the layers that operate on the higher resolution like a residual block, whose weight α increases linearly from 0 to 1. Here $2\times$ and $0.5\times$ refer to doubling and halving the image resolution using nearest neighbor filtering and average pooling, respectively. The toRGB represents a layer that projects feature vectors to RGB colors and fromRGB does the reverse; both use 1×1 convolutions. When training the discriminator, we feed in real images that are downsampled to match the current resolution of the network. During a resolution transition, we interpolate between two resolutions of the real images, similarly to how the generator output combines two resolutions.

(Karras et al, 2017)



Progressive Growing of GANs for Improved Q...



Watch later



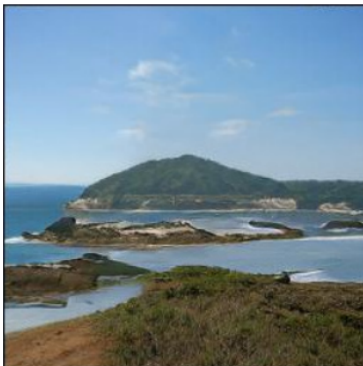
Share



(Karras et al, 2017)

BigGANs

Self-attention GANs as baseline (Zhang et al, 2018) + Hinge loss objective (Lim and Ye, 2017; Tran et al, 2017) + Class information to g with class-conditional batchnorm (de Vries et al, 2017) + Class information to d with projection (Miyato and Koyama, 2018) + Half the learning rate of SAGAN, 2 d -steps per g -step + Spectral normalization for both g and d + Orthogonal initialization (Saxe et al, 2014) + Large minibatches (2048) + Large number of convolution filters + Shared embedding and hierarchical latent spaces + Orthogonal regularization + Truncated sampling + (quite a few other tricks)



(Brock et al, 2018)



The 1000 ImageNet Categories inside of BigG...



Watch later



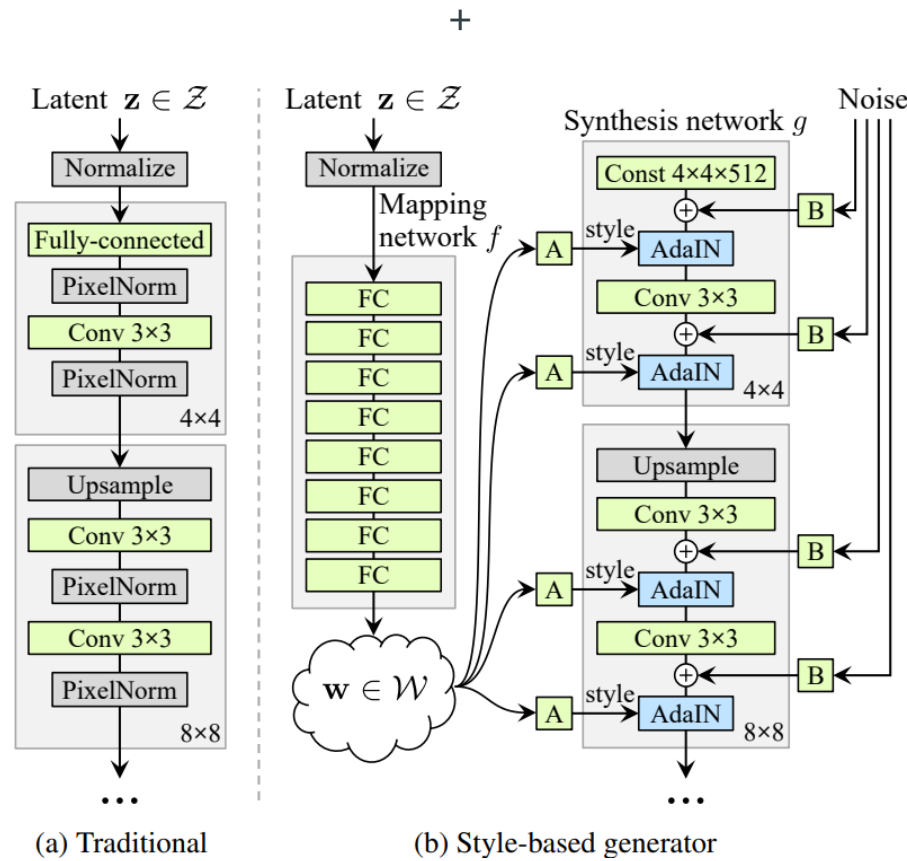
Share



(Brock et al, 2018)

StyleGAN

Progressive GANs as baseline (Karras et al, 2017) + Non-saturating loss instead of WGAN-GP + R_1 regularization (Mescheder et al, 2018) + (quite a few other tricks)



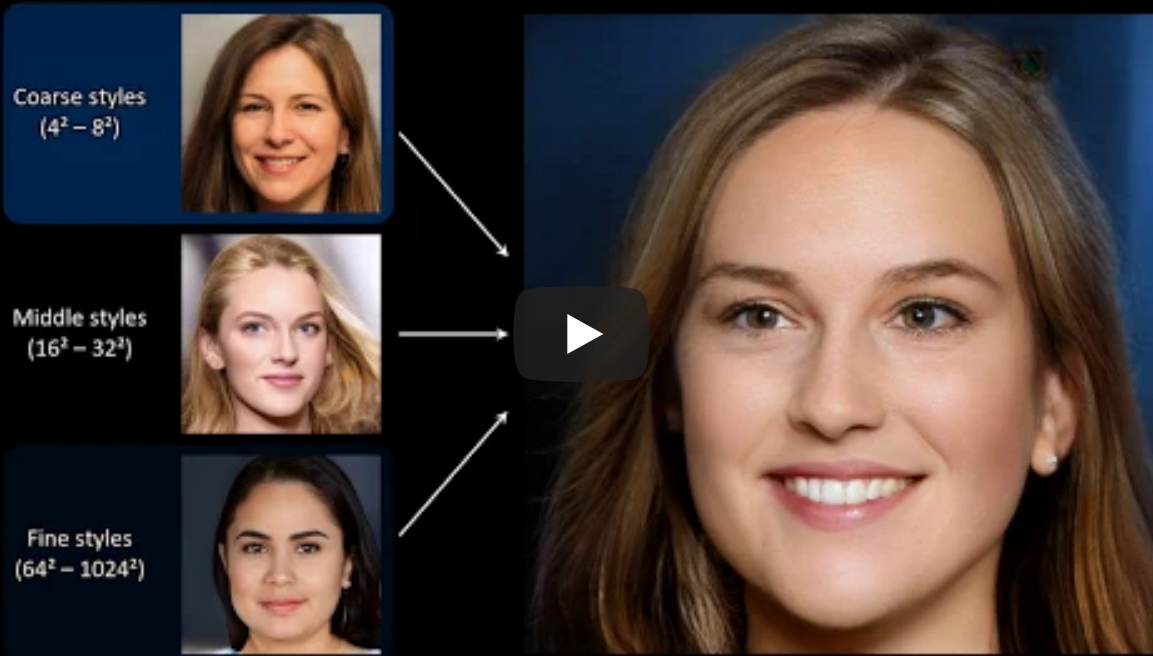


A Style-Based Generator Architecture for Gen...



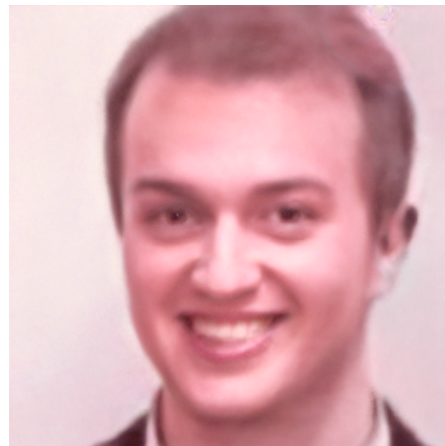
Watch later

Share



(Karras et al, 2018)

The StyleGAN generator g is so powerful that it can re-generate arbitrary faces.



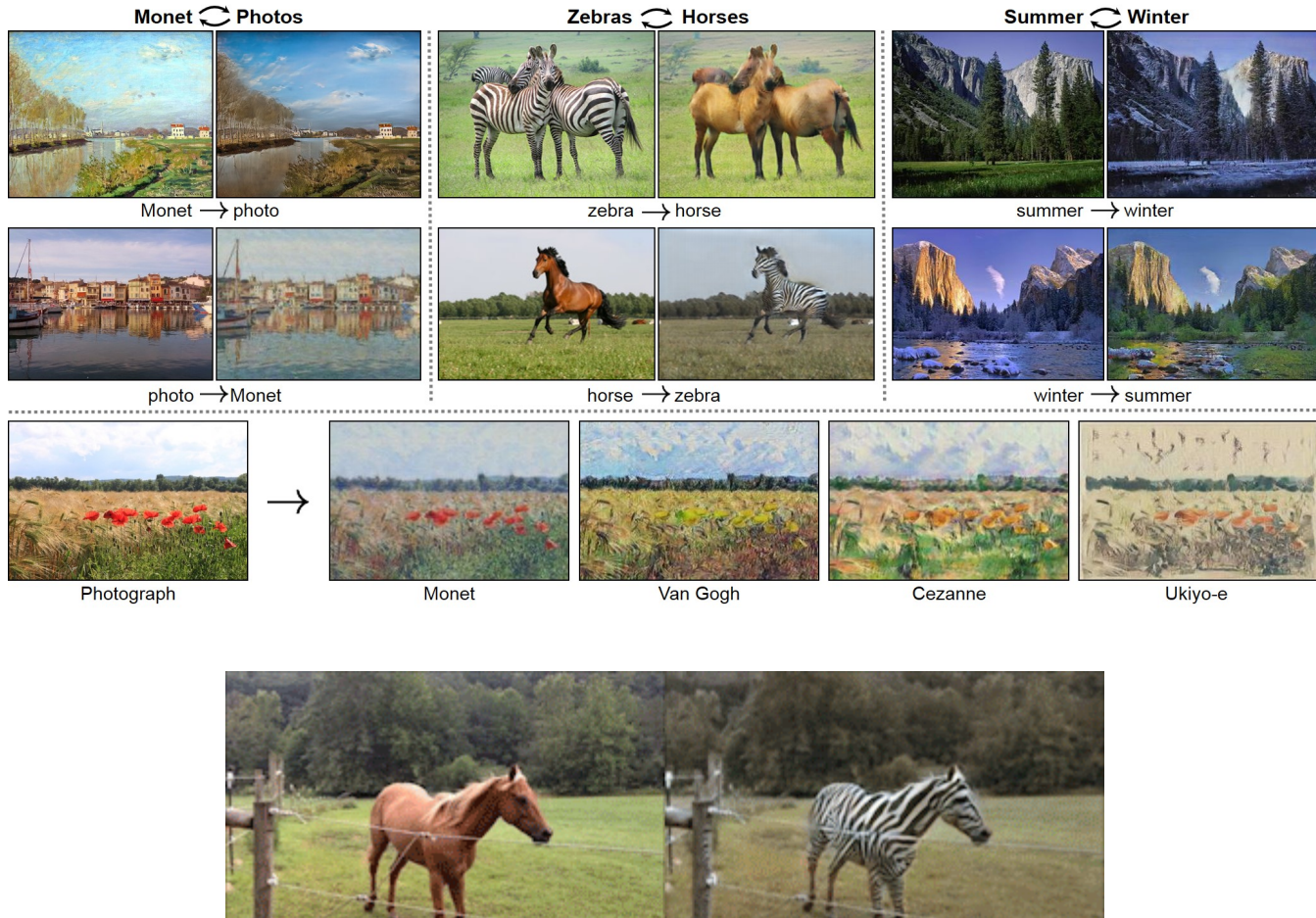




Applications

$p(\mathbf{z})$ need not be a random noise distribution.

Image-to-image translation



CycleGANs (Zhu et al, 2017)



Changing Sketches into Photorealistic Master...



Watch later

Share



GauGAN: Changing sketches into photorealistic masterpieces (NVIDIA, 2019)



High-Resolution Image Synthesis and Semant...



Watch later



Share



High-resolution image synthesis (Wang et al, 2017)

Captioning



a tennis player gets ready to return a serve



two men dressed in costumes and holding tennis rackets



a tennis player hits the ball during a match



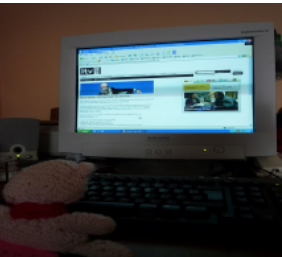
a male tennis player in action on the court



a man in white is about to serve a tennis ball



a laptop and a desktop computer sit on a desk



a person is working on a computer screen



a cup of coffee sitting next to a laptop



a laptop computer sitting on top of a desk next to a



a picture of a computer on a desk

(Shetty et al, 2017)

Text-to-image synthesis

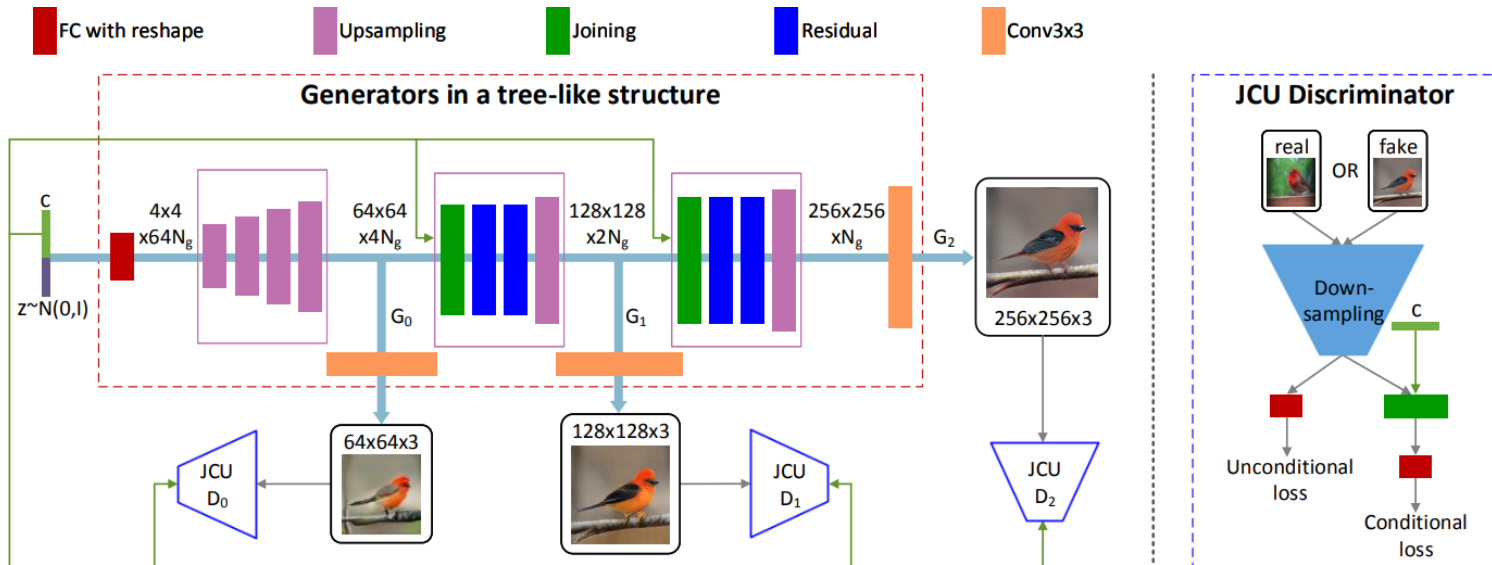


Fig. 2: The overall framework of our proposed StackGAN-v2 for the conditional image synthesis task. c is the vector of conditioning variables which can be computed from the class label, the text description, etc.. N_g and N_d are the numbers of channels of a tensor.

(Zhang et al, 2017)

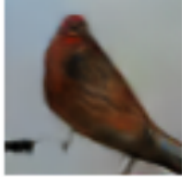
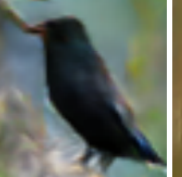
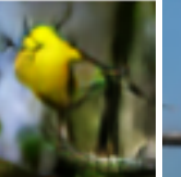
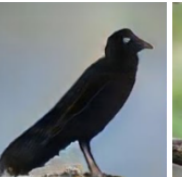
Text description	This bird is red and brown in color, with a stubby beak	The bird is short and stubby with yellow on its body	A bird with a medium orange bill white body gray wings and webbed feet	This small black bird has a short, slightly curved bill and long legs	A small bird with varying shades of brown with white under the eyes	A small yellow bird with a black crown and a short black pointed beak	This small bird has a white breast, light grey head, and black wings and tail
64x64 GAN-INT-CLS							
128x128 GAWWN							
256x256 StackGAN-v1							

Fig. 3: Example results by our StackGAN-v1, GAWWN [29], and GAN-INT-CLS [31] conditioned on text descriptions from CUB test set.

(Zhang et al, 2017)

Music generation

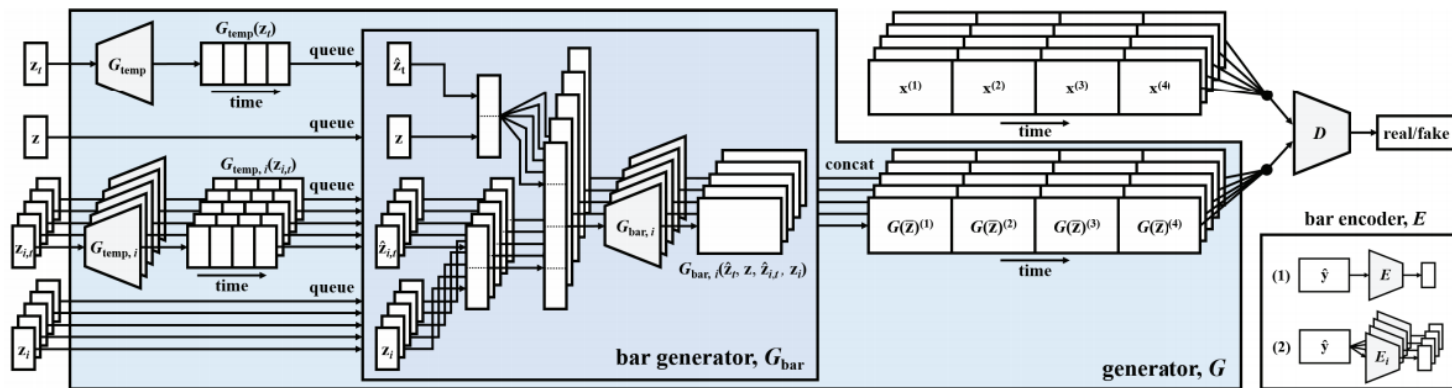


Figure 5: System diagram of the proposed MuseGAN model for multi-track sequential data generation.

▶ 0:00 / 3:15 ● 🔊

MuseGAN (Dong et al, 2018)

Accelerating scientific simulators

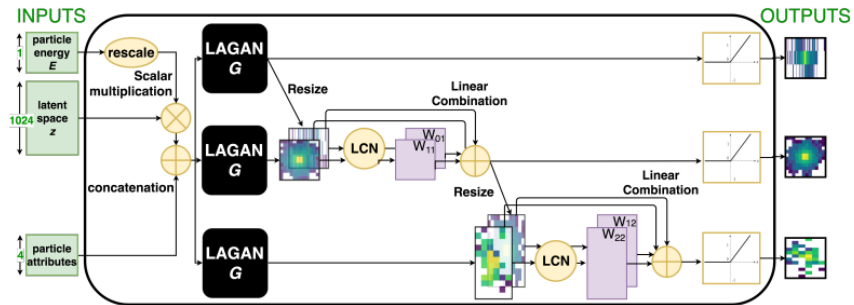


Figure 8.37: Composite conditional CaloGAN generator G , with three LAGAN-like streams connected by attentional layer-to-layer dependence.

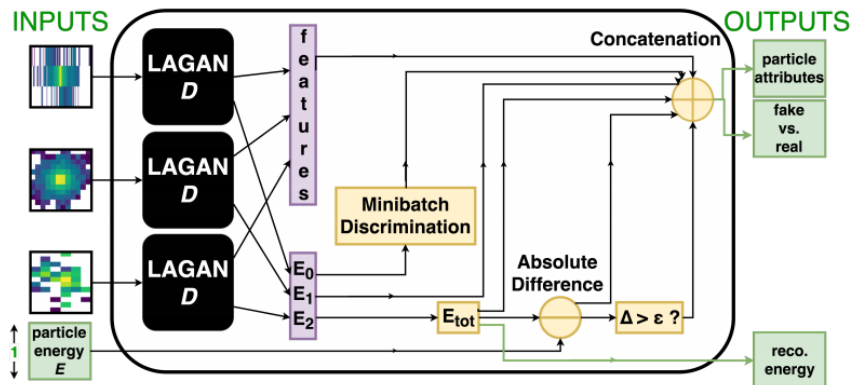
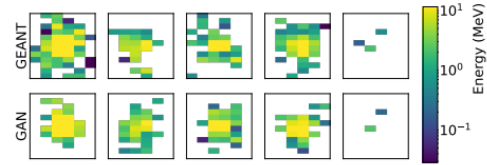
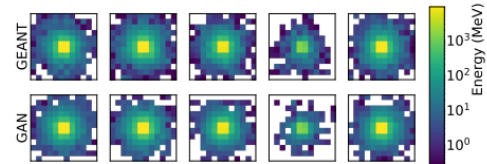
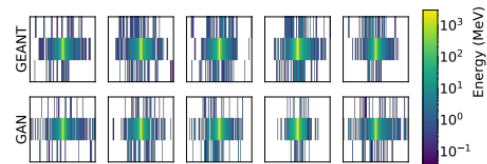


Figure 8.38: Composite conditional CaloGAN discriminator D , with three LAGAN-like streams and additional domain-specific energy calculations included in the final feature space.



Learning particle physics (Paganini et al, 2017)

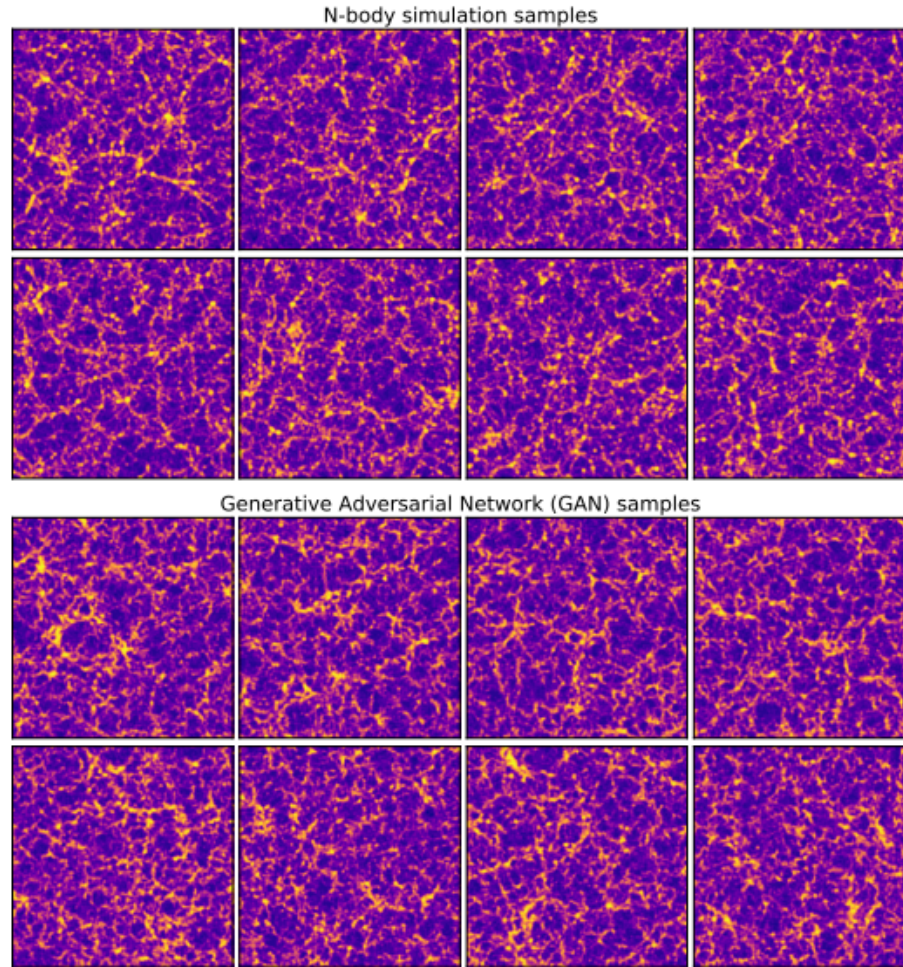
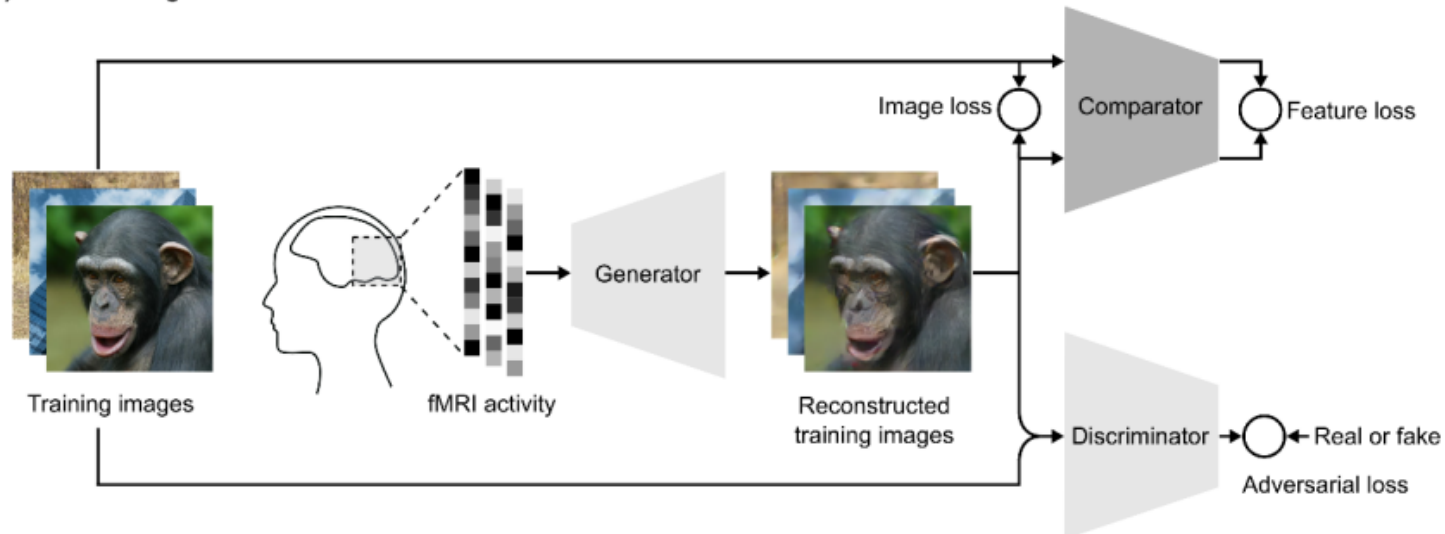


Figure 1: Samples from N-body simulation and from GAN for the box size of 500 Mpc. Note that the transformation in Equation 3.1 with $a = 20$ was applied to the images shown above for better clarity.

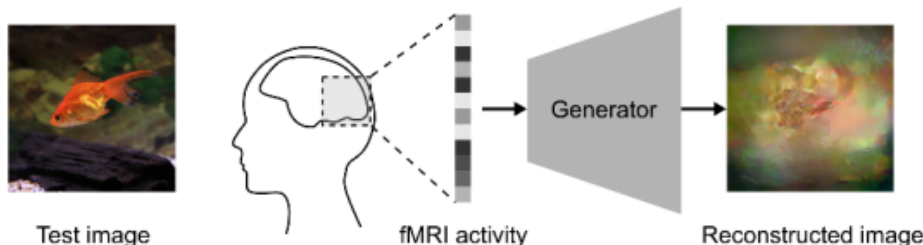
Learning cosmological models (Rodriguez et al, 2018)

Brain reading

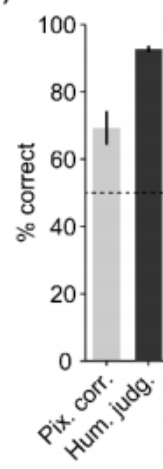
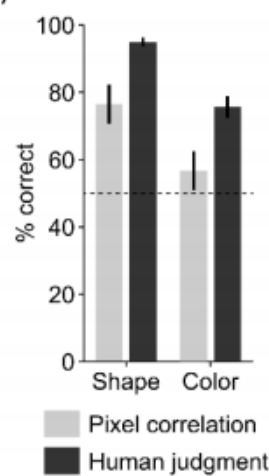
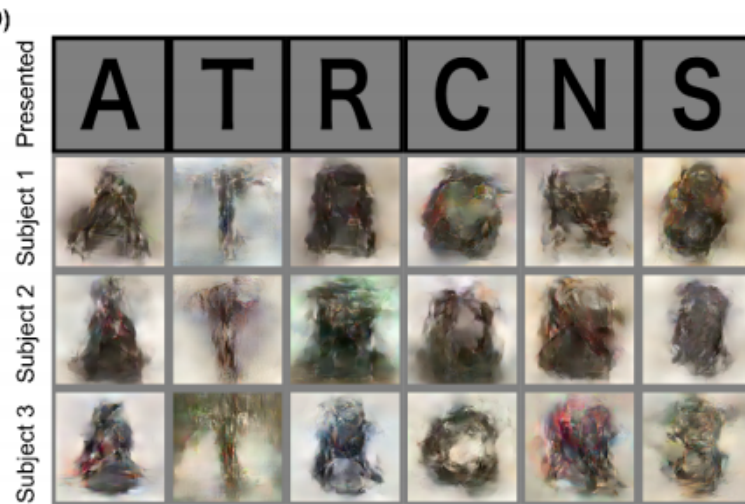
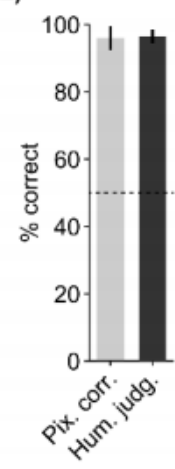
(A) Model training



(B) Model test



(Shen et al, 2018)

(A)**(B)****(C)****(D)****(E)**

(Shen et al, 2018)



Deep image reconstruction: Natural images



Watch later



Share



Brain reading (Shen et al, 2018)

The end.

References

- Goodfellow, I., Pouget-Abadie, J., Mirza, M., Xu, B., Warde-Farley, D., Ozair, S., ... & Bengio, Y. (2014). Generative adversarial nets. In Advances in neural information processing systems (pp. 2672-2680).
- Arjovsky, M., Chintala, S., & Bottou, L. (2017). Wasserstein gan. arXiv preprint arXiv:1701.07875.
- Mescheder, L., Geiger, A., & Nowozin, S. (2018). Which training methods for GANs do actually Converge?. arXiv preprint arXiv:1801.04406.